Stony Brook University

Expression, Purification, and Characterization of the Short Isoform of Human Adenylosuccinate Lyase

A Thesis Presented

by

Benjamin Rajan

to

The Graduate School

In Partial Fulfillment of the

Requirements

for the Degree of

Master of Science

in

Biochemistry and Cell Biology

Stony Brook University

December 2014

Stony Brook University

The Graduate School

Benjamin Rajan

We, the thesis committee for the above candidate for the

Master of Science degree, hereby recommend

acceptance of this thesis.

Dr. Jarrod B. French, Ph.D. – Thesis Advisor
Assistant Professor, Departments of Chemistry and Biochemistry & Cell Biology

Dr. Steven E. Glynn, Ph.D. – Second Reader
Assistant Professor, Department of Biochemistry & Cell Biology

This thesis is accepted by the Graduate School

Charles Taber
Dean of the Graduate School

Abstract of the Thesis

Expression, Purification, and Characterization of the Short Isoform of Human Adenylosuccinate Lyase

by

Benjamin Rajan

Master of Science

in

Biochemistry and Cell Biology

Stony Brook University

2014

Cells require purines for critical biological processes that can be created by the *de novo* biosynthetic pathway or maintained by the salvage pathways. The *de novo* pathway in humans requires 6 enzymes, some of which are multifunctional. Adenylosuccinate lyase (ASL) catalyzes step 8 of the *de novo* pathway converting susuccinylaminoimidazolecarboxamide ribonucleotide (SAICAR) to aminoimidazolecarboxamide ribotide (AICAR). It also catalyzes the second step of the purine nucleotide cycle by converting SAMP to AMP. A short isoform of ASL (sASL) is ubiquitously expressed in all cell types at a lower concentration. This shortened splice variant does not perform catalysis on either of the aforementioned substrates. It has been suggested that sASL may play an important structural role in the formation and stabilization of the purinosome assembly. The purpose of this work is to characterize the short isoform of ASL and elucidate its structure and function. To date, I have cloned sASL, expressed and purified the protein, and identified a buffer that stabilizes it.

Table of Contents

List of Figures

List of Tables

List of Abbreviations

αKG	α-ketoglutarate
Aβ	Beta amyloid peptide
ADE12	Yeast homolog of adenylosuccinate lyase
AMP	Adenosine monophosphate
ASA	Mixed heteromeric short and long isoforms of adenylosuccinate lyase
ASL	Adenylosuccinate lyase
AICAR	Aminoimidazolecarboxamide ribotide
ATP	Adenosine triphosphate
ATIC	Bifunctional aminoimidazolecarboxamide ribonucleotide transformylase and inosine monophosphate cyclohydrolase
cGMP	Cyclic guanosine monophosphate
cAMP	Cyclic adenosine monophosphate
CD	Circular dichroism
CREB	Cyclic-AMP response element binding protein
CtpS	CTPase synthetase
FAD	Flavin adenine dinucleotide
FGAMS	Formylglycinamide ribonucleotide synthetase
FPLC	Fast protein liquid chromatography
GMP	Guanosine monophosphate
GTP	Guanosine triphosphate
HPRT	Hypoxanthine phosphoribosyl transferase
Hsp	Heat shock protein

IMAC	Immobilized metal affinity chromatography
IMP	Inosine monophosphate
IPTG	Isopropyl β-D-1-thiogalactopyranoside
MPD	Hexylene glycol
NAD^+	Nicotinamide adenine dinucleotide
NADP	Nicotinamide adenine dinucleotide phosphate
PAGE	Polyacrylamide gel electrophoresis
PAICS	Bifunctional carboxyaminoimidazole ribonucleotide synthase and susuccinylaminoimidazolecarboxamide ribonucleotide synthetase
PKA	Phosphokinase A
PPAT	Phosphoribosylpyrophosphate amidotransferase
PRPP	Phosphoribosylpyrophosphate
SAICAR	Susuccinylaminoimidazolecarboxamide ribonucleotide
SAMP	Adenylosuccinate
sASL	Short isoform of adenylosuccinate lyase
SDS	Sodium dodecyl sulfate
SEC	Size exclusion chromatography
TGART	Trifunctional glycinamide ribonucleotide synthetase, glycinamide ribonucleotide transformylase, and aminoimidazole ribonucleotide synthetase

Introduction

Purines are critical components needed for various cellular functions from synthesizing DNA and RNA to the formation of high energy molecules. These necessary molecules are maintained in the cell by two pathways known as the *de novo* biosynthetic pathway and the salvage pathway. Step eight of the biosynthetic pathway is catalyzed by adenylosuccinate lyase. A short isoform of this enzyme is expressed in all tissue types, yet it has no catalytic function and is largely uncharacterized. This work will elucidate important features of the regulation of purine biosynthesis and help provide insights into the role of this short isoform and how it may act to control the structure and function of the purinisome.

Role of Purines and its Derivatives

A purine (1) is a nitrogen containing heterocyclic aromatic compound, with basic properties, that consists of a five member ring and a six member ring fused together. Purines and its derivatives are necessary for all life and are involved in numerous metabolic processes. Purines are needed as bases for nucleoside triphosphates in DNA replication and RNA synthesis, they are used in high energy molecules, as signaling molecules, and also as cofactors. The class of purines includes adenine (2), guanine (3), hypoxanthine (4), xanthine (5), theobromine (6), isoguanine (7), and caffeine (8) to name a mere handful. Purines and the large chemodiversity of its derivatives create a massive resource for new lead structures for medicinal chemistry [1]. Purine analogs and clinical anti-metabolites that are targeted against the enzymes that create purines are used as chemotherapeutics to combat cancer. Purines play an important role in multiple cellular functions and the intricate balance of intra and extracellular purines requires a high degree of regulation. Along with serving a biological function, purine derivatives have also

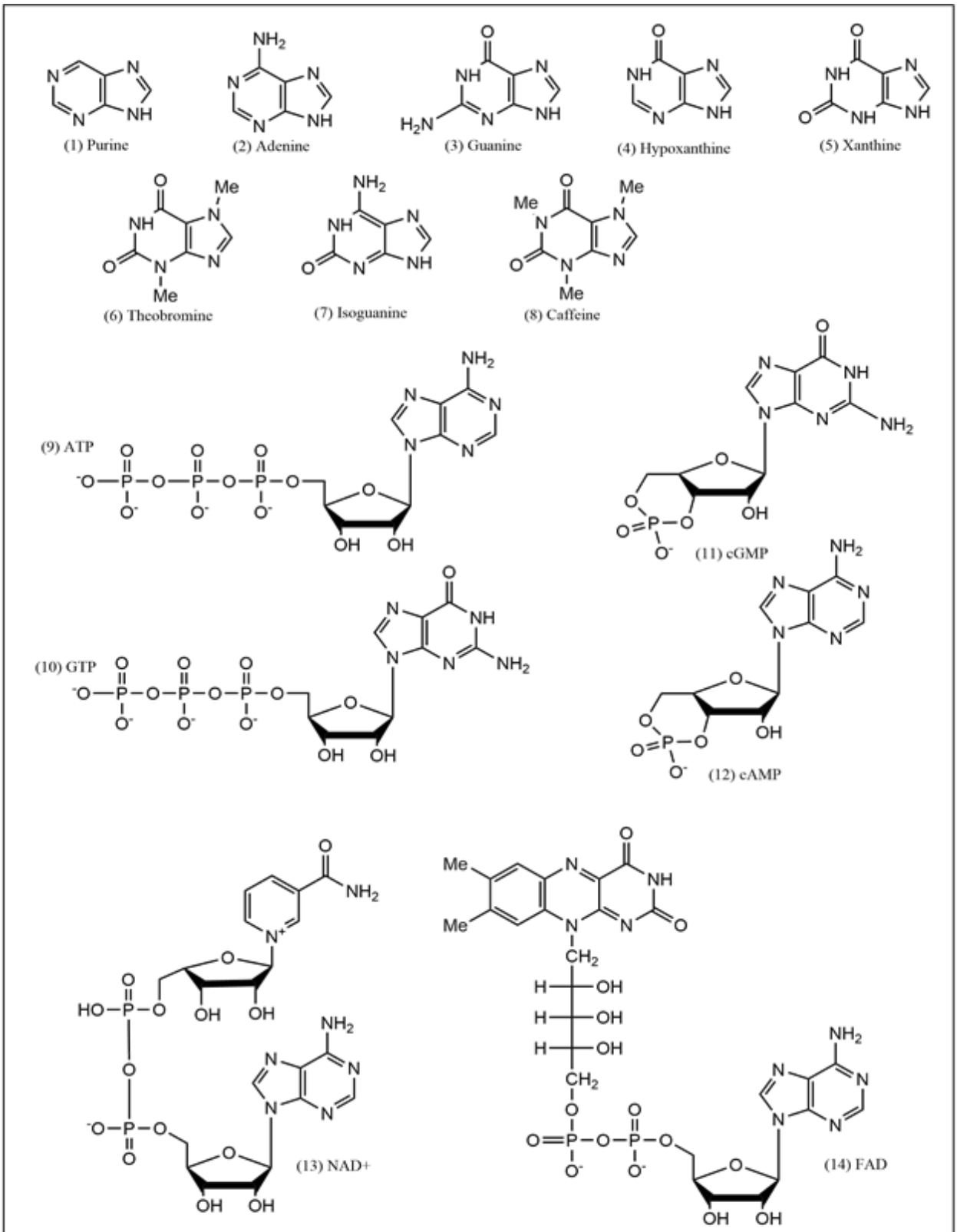

Figure 1. Purine and its derivatives. Show is a purine and its various derivatives, including the high energy molecules ATP and GTP, second messengers cAMP and cGMP, and cofactors NAD+/NADH and FAD. All structures created in ChemDraw.

been used in the food industry [1]. Nucleotides are naturally occurring tastants that, when mixed with other salts, produce a desirable, enhancing flavor [2].

Purines in Extracellular Signaling

Extracellular purines can act as messengers in what is referred to as purinergic signaling. Adenosine was first introduced as an extracellular signaling molecule by observing its ability to decrease heart rate and increase coronary blood flow [3] and has since been found to have regulatory roles in nearly every organ system [4]. Adenosine is used as a diagnostic agent to assess coronary artery function together with radionuclide myocardial perfusion imaging [5], during which the blood supply and flow to the heart is monitored. Adenosine represents a pre-eminent alarm system as it accumulates in the extracellular space in response to metabolic stress or cell damage. Activation of adenosine receptors has been shown to modulate the immune system and inflammatory response [4]. Adenosine receptors are divided into four subcategories that are coupled via different G proteins to activate phospholipase C or adenylyl cyclase. Therapeutic approaches include adjusting the concentration of extracellular adenosine and moderating receptor activity.

ATP and GTP

Adenosine triphosphate (ATP; 9) is one of the most widely known purine derivatives. It is used as the universal energy storage molecule in all living cells and the free energy available from hydrolyzing the high energy phosphate bond is used to drive energy requiring reactions [6]. ATP functions as an extracellular signaling mediator in numerous biological processes [7]. Sensory mechanisms measure and monitor the internal states within every organism. Any change in that

internal environment, including ATP levels, leads to a behavioral or physiological response [7]. Guanosine triphosphate (GTP; 10), another purine derivative that is much like ATP, is best known for its involvement in RNA synthesis, the citric acid cycle, and as an energy source for protein synthesis. Guanosine monophosphate (GMP) acts as an intermediate in the synthesis of nucleic acids and plays important roles in metabolic processes [8]. Changes in local purine nucleotide and nucleoside concentrations can affect phagocytosis, cytokine release, result in proliferation, facilitate blood coagulation, and control cytotoxicity [9, 10].

ATP Receptors and Extracellular Signaling

Reports have highlighted the involvement of ATP in extracellular signaling within host-tumor interactions [11]. Nucleotide receptors are divided into two families, P2X and P2Y receptors [12], which are widely distributed across animal species and ubiquitously expressed on both excitable and non-excitable mammalian cells. In addition, ATP is the only physiological ligand of P2X receptors that has been identified thus far [11] and plays a role in interleukin-1β release, antigen presentation, and lymphocyte proliferation and differentiation [13, 14].

Physiological Relevance of Purine Signaling in the Nervous System

In the peripheral nervous system, there is a common mechanism that innervates sensory neurons via the P2X and P2Y receptors using ATP as the signaling molecule [15]. During nociception, when the body feels a painful stimulus, cytosolic ATP is released from damaged cells into the extracellular space which activates receptors and results in the perception of pain [16]. ATP signaling also plays a role in micturition, when stored urine is released, during epithelial stretch of the bladder [17]. Chemosensors in the carotid artery are responsible for measuring the

oxygen content of the blood. Oxygen sensitive cells release ATP as an extracellular signaling molecule which activates P2X receptors on the carotid sinus nerve and transmits relevant information about the partial oxygen pressures to the areas of the brain responsible for respiration [18]. In addition to the peripheral nervous system, it has been reported that ATP can convey sensory information when released at the chemosensitive areas of the central nervous system which can moderate breathing [7]. Furthermore, it has been suggested that adenosine plays an important role in ischemia, which is when a blockage of blood flow occurs and the metabolic needs of a tissue exceed the available supply of oxygen. As mentioned previously, adenosine can induce vasodilation by producing a relaxing effect on vascular smooth muscle that is independent of nitric oxide release, which is typically associated with vasodilation, and also independent of the surrounding endothelium tissue [19].

Purines as Second Messengers

Cyclic guanosine monophosphate (cGMP; 11) is a second messenger molecule generated from GTP that can cause the relaxation of smooth muscle surrounding blood vessels, decrease platelet aggregation, and make alterations in neuron function that affect memory and behavior [20]. Cyclic adenosine monophosphate (cAMP; 12), which is generated at the cell membrane by adenylyl cyclase using ATP, functions as another second messenger molecule that initiates a cascade of intracellular events by activating protein kinases and controlling ion concentrations. cAMP is involved in activating cyclic-AMP response element binding protein (CREB) which is a known transcription factor that participates in gene transcription [21]. cAMP signaling requires phosphokinase A (PKA), anchored at the membrane [22, 23], which is responsible for turning on multiple downstream signaling pathways. Its activity is sequestered by cyclic nucleotide

phosphodiesterases that act to create a functional barrier to cAMP diffusion [22]. cAMP can also function as a pro-apoptotic and anti-apoptotic second messenger. Its ability to activate PKA can lead to apoptosis or cell survival [23].

Purine Nucleotides as Cofactors

Another important function of purines is its role in cofactors used in various metabolic processes. Nicotinamide adenine dinucleotide (NAD^+; 13) and flavin adenine dinucleotide (FAD; 14) are both purine coenzymes known for their involvement in oxidation and reduction reactions within the biological systems. NAD^+ and NADH (reduced) are the key primary charger carriers that shuttle hydrogen atoms and electrons from one metabolite to another in the electron transport chain. It is also used as a cofactor in a large number of dehydrogenase enzymatic reactions [24]. $NADP^+$ and NADPH (reduced), also purine coenzymes, differ from NAD^+ by the addition of a phosphate group and are best known for their involvement in the light reactions of photosynthesis as well as the pentose phosphate pathway in non-photosynthetic organisms. Another important coenzyme, acetyl-coenzyme A, is a purine containing molecule used in particular biological processes such as oxidation of pyruvate and in fatty acid metabolism [25].

Purine Biosynthesis

Enzyme Clustering

Many important cellular metabolites are generated by multi-step pathways that are composed of several distinct enzymes. Regulation of these pathways and conversion from substrate to product is tightly controlled in order to maintain metabolite levels. The cell has a number of mechanisms intended to increase flux through the pathway and to control a multi-step

process. Intermediates within a multi-enzyme pathway can rapidly diffuse throughout the cell cytoplasm before finding the active site of the next enzyme. In order to increase efficiency and flux of substrate to final product, a phenomena known as direct channeling can occur [26]. Direct channeling requires the formation of a physical protein tunnel that connects consecutive active sites together. This connection prevents the intermediate from escaping in transit. Substrates can be shuttled from one active site of one enzyme to the active site of another enzyme or from one active site to another active site on the same polyfunctional enzyme [27]. Proximity channeling occurs when an intermediate diffuses from one enzyme to another nearby enzyme in the absence of a physical protein channel. For this to occur, the enzymes must be co-localized and are typically found on protein scaffolds [28]. A fundamental issue exists for the proximity channeling model—scaffolds increase metabolic yield, but do not bring enzymes close enough together for this kind of proximity channeling processing to be effective. Due to random diffusion, it is unlikely that an intermediate would be able to proceed from the first active site to the second active site without a driving force. It has been suggested that a possible solution to this issue could involve functional co-clustering of the enzymes in what is referred to as an agglomerate. This kind of compact agglomerate of enzymes in cluster-mediated channeling gives the same advantages as direct channeling, such as an increased flux in intermediate processing, as a result of higher enzyme concentration in a given region [26]. Essentially, the enzymes of a particular multi-enzyme pathway are present at high concentrations in the same region of space giving rise to increased efficiency and flux. Evidence for enzyme clustering has been observed in several organisms [29-33]. As recent evidence has shown, the clustering of enzymes in a defined region of space can cause shunting of intermediates from one branch point of a pathway to another depending on the cluster of enzyme present, resulting in an effective means of controlling the directionality of

metabolic flux [26]. Enzyme clustering with many copies of another subsequent enzyme increases intermediate processing and subsequently increases metabolic efficiency of pathways that have unstable intermediates [34]. Synthetically engineering these clusters has demonstrated that the acceleration of intermediate processing is a direct result of enzyme agglomerate formation without a defined specific microscopic arrangement of the enzymes [26].

Purine Biosynthetic and Salvage Pathways

Purines are essential building blocks used for various biological processes. As mentioned before, ATP is used as the primary energy storage molecule and so a steady supply of ATP is needed for metabolically active cells. The ratio of ATP to ADP and AMP is thermodynamically more important than the absolute concentration of ATP [6]. Rapidly dividing cells also have a high demand for purines that are needed as raw material for DNA replication, RNA synthesis, high energy molecules, and signaling molecules. Cells have the ability to create purines in two ways: the *de novo* biosynthetic pathway and the salvage pathway. These pathways are responsible for generating and maintaining cellular levels of inosine monophosphate (IMP) (**Figure 2**) and subsequently levels of AMP and GMP. The salvage pathway catalyzes the one-step conversion of hypoxanthine to IMP by hypoxanthine phosphoribosyl transferase (HPRT) (**Figure 3**) [35]

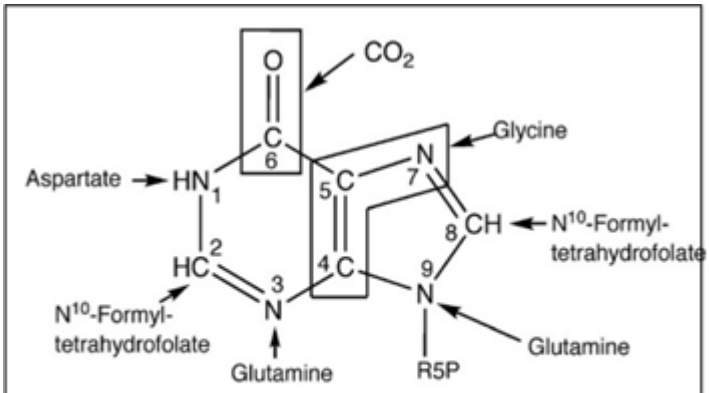

Figure 2. Inosine monophosphate. Shown above are the precursors of inosine monophosphate. R5P stands for the sugar ribose 5'-phosphate.

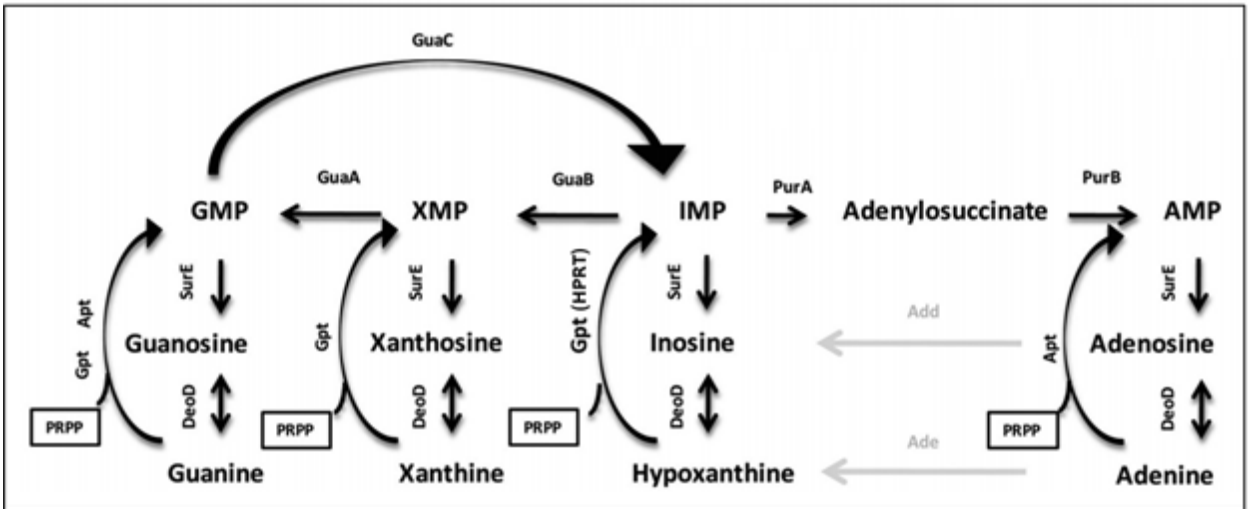

Figure 3. Purine salvage pathway. Shown is the salvage pathway in *H. pylori* that depicts the conversion of IMP to various products and back again. The purine salvage pathway is the predominate method to maintain the purine pool. HPRT catalyzes the conversion of hypoxanthine to IMP in a single step. PurB, also known as ASL in humans, converts SAMP to AMP [35].

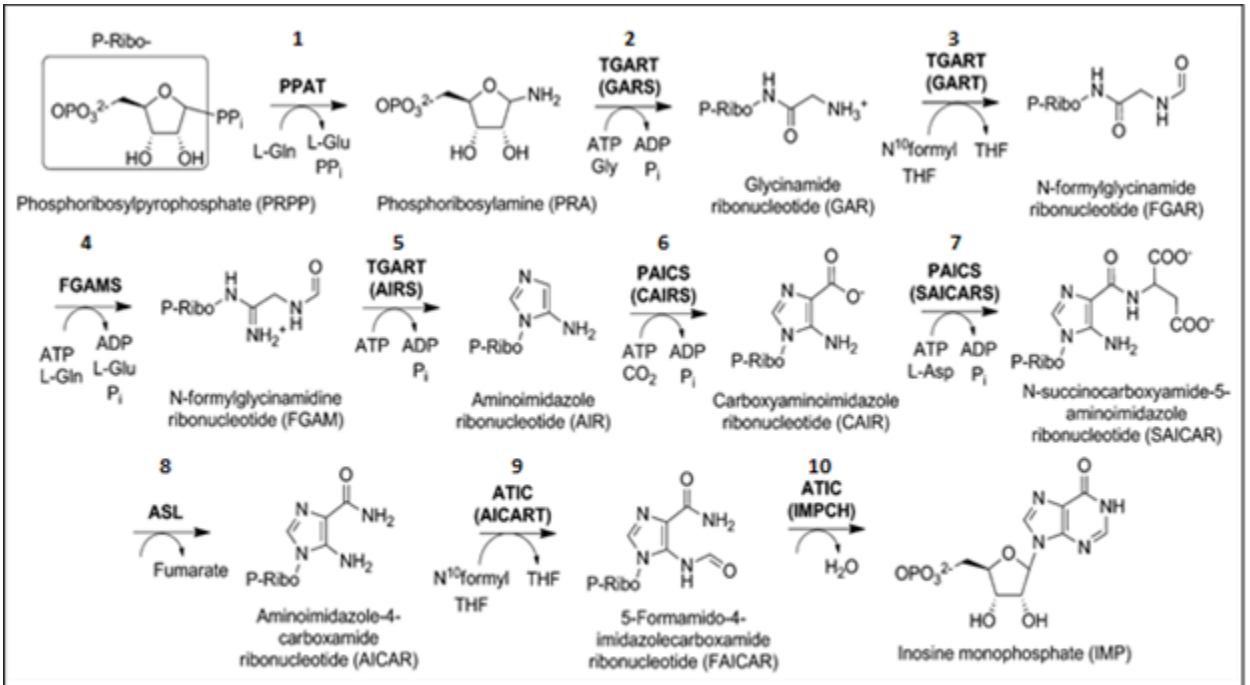

Figure 4. The 10 conserved enzymatic steps of the *de novo* purine biosynthetic pathway. Six enzymes that carry out purine biosynthesis in humans: PPAT, TGART, FGAMS, PAICS, ASL and ATIC. Starting material is PRPP and ends with IMP [36].

whereas the *de novo* pathway exhibits tighter control and regulation and consists of 10 conserved chemical reactions that convert phosphoribosylpyrophosphate (PRPP) to IMP (**Figure 4**) [34]. In

prokaryotes, the pathway is catalyzed by 10 separate enzymes. In humans, this number has been reduced to six gene products, including one trifunctional enzyme and two bifunctional enzymes [36]. The *de novo* pathway can be regulated by allosteric inhibition of the first, rate limiting enzyme by the downstream products AMP and GMP [37-39]. Both pathways are always active; however, when purine requirements are high, such as in rapidly dividing cells, the biosynthetic pathway is upregulated to meet the demand. Under normal conditions, the purine salvage pathway is sufficient to provide enough raw material for the cell. Rapidly dividing cells, such as in cancers, are heavily dependent on the *de novo* pathway while non-proliferating cells can survive on the purines maintained by the salvage pathway. The redundancy of having two pathways, makes the *de novo* biosynthetic pathway an important target for anticancer, antiviral, and antimicrobial drug development [40].

The Purinosome

In humans, there are six enzymes that catalyze the 10 steps of the *de novo* biosynthesis of purines: PPAT, TGART, FGAMS, PAICS, ASL, and ATIC. Phosphoribosylpyrophosphate amidotransferase (PPAT) catalyzes the first step of the pathway. TGART, the trifunctional enzyme, is composed of glycinamide ribonucleotide synthetase (GARS), glycinamide ribonucleotide transformylase (GART), and aminoimidazole ribonucleotide synthetase (AIRS). TGART catalyzes nonsequential steps 2, 3, and 5. Formylglycinamide ribonucleotide synthetase (FGAMS) catalyzes step 4. PAICS, a bifunctional enzyme, is composed of carboxyaminoimidazole ribonucleotide synthase (CAIRS) and susuccinylaminoimidazolecarboxamide ribonucleotide synthetase (SAICARS), which catalyzes steps 6 and 7, respectively. Adenylosuccinate lyase (ASL) catalyzes step 8. ATIC, composed of

aminoimidazolecarboxamide ribonucleotide transformylase (AICARTfase) and the inosine monophosphate cyclohydrolase (IMPCH), catalyzes steps 9 and 10, respectively.

These enzymes were observed to reversibly form clusters dependent on purine demand [34, 41]. Enzymes of this pathway have been co-purified from native source tissues that indicate a level of interaction between several of the proteins [33]. FGAMS is believed to interact with TGART, which would minimize random diffusion of the intermediate between steps 3, 4, and 5. FGAMS is an established marker for observing the localization of the other members of the pathway and it is also speculated to be the scaffold for the formation of the purinosome [29, 34]. The purinosome is a proposed agglomerate of enzymes that come together to perform the aforementioned enzymatic steps of the *de novo* pathway that produces IMP from the starting material, PRPP, while consuming 5 molecules of ATP.

Purinosome Formation

This purinosome cluster forms in response to the availability of purines and its demand within the cell. Work has been conducted showing that, under purine rich conditions, the members of the purinosome exhibit diffuse cytoplasmic distributions, whereas in purine depleted conditions, cytoplasmic clustering of all six of the human *de novo* biosynthetic enzymes is observed [34]. This suggests that the clustering of the purinosome is tied to a cellular sensor that detects an insufficient levels of purines. Purinosome formation appears to be a general phenomenon in all cell types during specific states of the cell cycle [34]. Formation of the purinosome appears to be tied with functional microtubules. Nocodazole is a drug known to depolymerize microtubules. When nocodazole is administered to a cell, the clustering of purinosome enzymes does not occur, even under purine deficient conditions [41]. This evidence

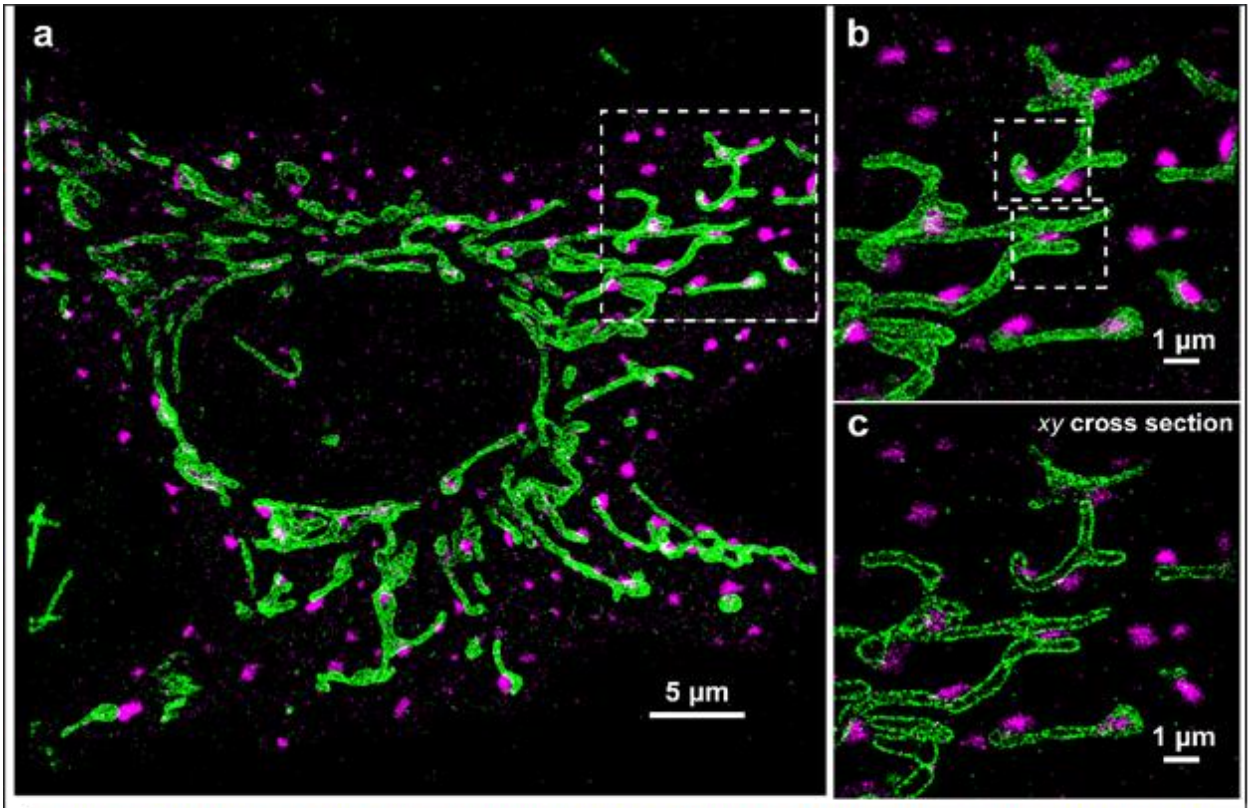

Figure 5. Purinosomes associating with mitochondria. (a) Super resolution image of purinosomes (FGAMS shown in magenta) and mitochondria (green). (b) A zoomed in view showing the tight association between the assembly and the organelle. (c) A xy-cross section that shows the purinosome and mitochondria are on the same axial plane in the cell [42].

suggests that the multienzyme purinosome complex associates with microtubules in the cytoplasm and that disruption of the microtubule network affects enzyme clustering and attenuates metabolic flux of *de novo* purine biosynthesis in purine depleted cells. Along with their association with microtubules, super resolution imaging has revealed that purinosomes closely interact with mitochondria (**Figure 5**). Purine biosynthesis is energy intensive and requires a high level of ATP. This tight association may be indicative of a synergistic relationship between purinosomes and mitochondria [42]. The cytoplasmic purinosome proteins ATIC, PAICS, and ASL have been found to co-purify with mitochondria without any chemical crosslinking, underscoring the level of physical interaction between the purinosome assembly and the organelle. In addition, it has been suggested that heat shock protein 70 (Hsp70) and heat shock protein 90 (Hsp90) help stabilize or

help assemble the purinosome. Hsp70 and Hsp90 are ubiquitously expressed chaperones that have been shown to be dynamically associate with the purinosome as the intracellular levels of purines change [36]. Addition of heat shock protein inhibitors or siRNA targeting these chaperones causes a knockdown and interrupts purinosome formation. It is important to note that the purinosome is present under normal conditions, not just when cellular levels of purines are depleted. Purinosome clusters are present in significantly higher quantities during purine starvation [29].

Adenylosuccinate Lyase

The human adenylosuccinate lyase (ASL) gene was first isolated by Fon et al. [43]. Full length human ASL is composed of 13 exons that span 23 kb, is 484 amino acids long, and is approximately 200 kDa. A truncated version of human ASL that is only 459 amino acids long was isolated by Stone et al. [44]. This truncation was a result of generating ASL cDNA from human liver starting at an alternative downstream starts site. Although it expressed well, it showed no enzymatic activity despite testing various other bacterial expression strains, buffer systems, purification methods, refolding

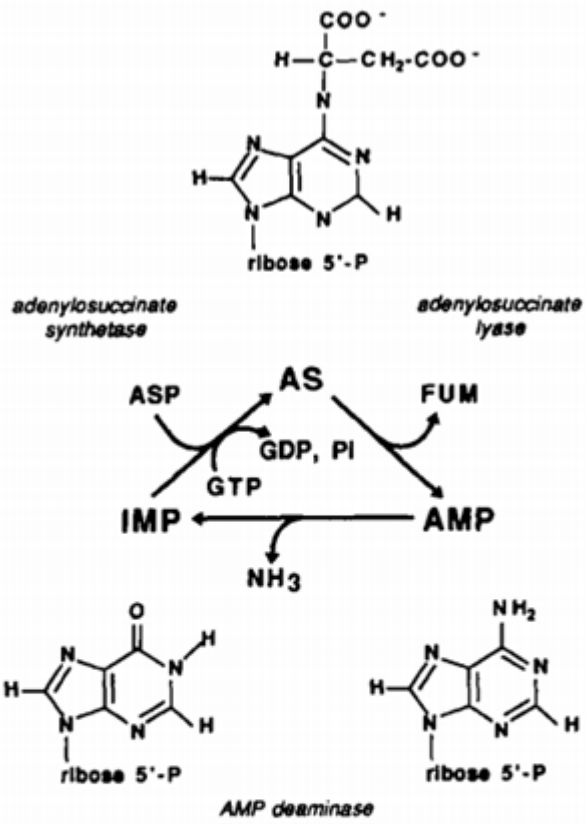

Figure 6. The purine nucleotide cycle. This cycle occurs after the 10 conserved steps in the *de novo* biosynthetic pathway, and converts IMP to AMP (IMP to GMP not shown). The conversion is carried out by adenylosuccinate synthetase, adenylosuccinate lyase (ASL), and AMP deaminase. In this figure, AS stands for adenylosuccinate (SAMP). The conversion of SAMP to AMP by ASL releases fumarate, a citric acid cycle intermediate [48].

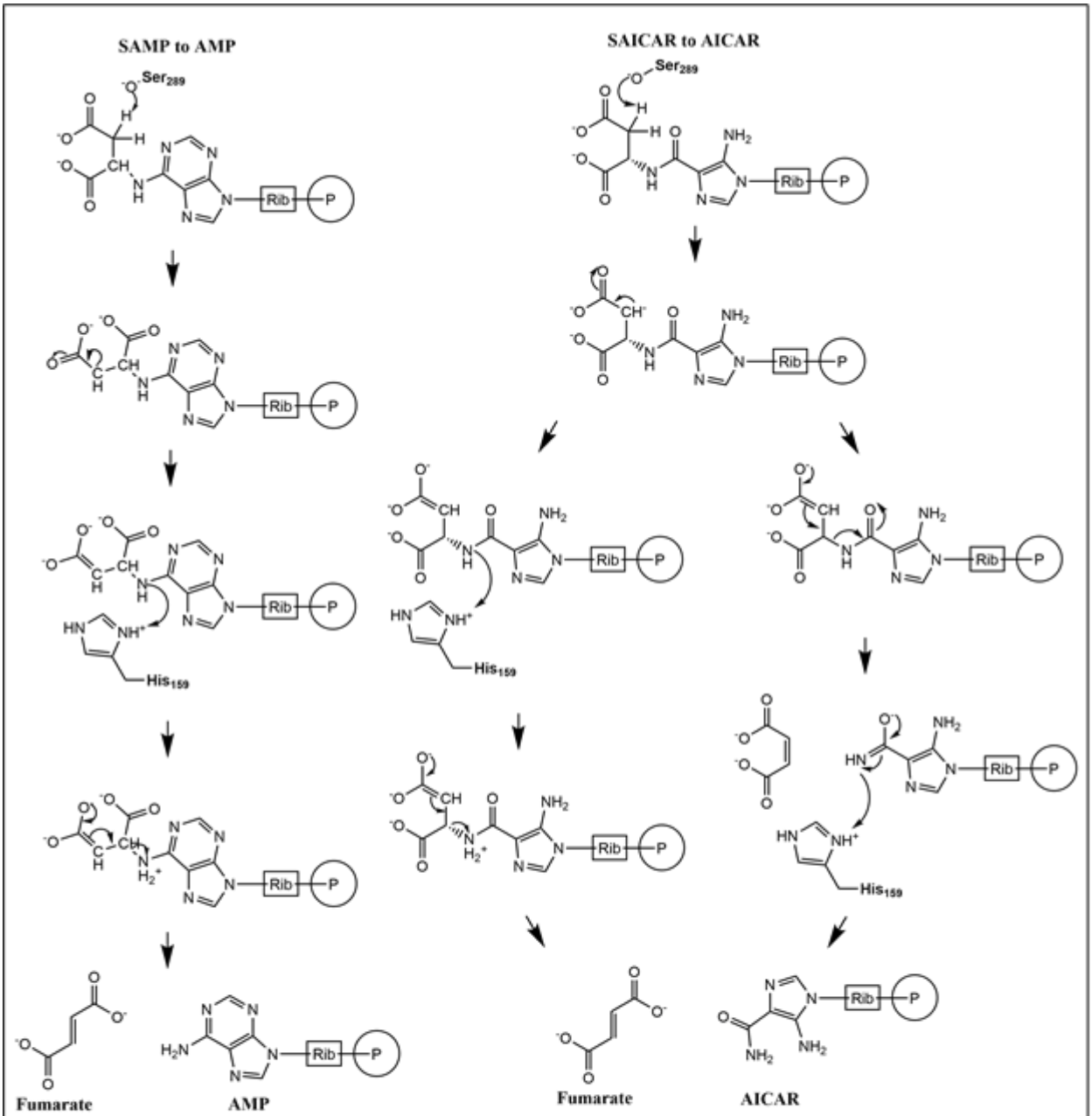

Figure 7. ASL catalytic mechanism. Above are the reactions catalyzed by human ASL in the *de novo* purine biosynthetic pathway (right) and subsequent purine nucleotide pathway (left). Shown are the proposed mechanisms to convert SAICAR to AICAR and fumarate and SAMP to AMP and fumarate. Ser289 and His159 are the suspected catalytic residues. Mechanism drawn in ChemDraw.

conditions, and cleavage of the 6xHis-tag [45]. ASL is a bifunctional enzyme that catalyzes two nonsequential steps: the eighth step of the purine *de novo* biosynthetic pathway, converting susuccinylaminoimidazolecarboxamide ribonucleotide (SAICAR) to

aminoimidazolecarboxamide ribonucleotide (AICAR), and the second step of the purine nucleotide cycle pathway (**Figure 6**), converting adenylosuccinate (SAMP) to adenosine monophosphate (AMP) [46-48]. Both of these β-elimination reactions lead to the release of fumarate [40] (**Figure 7**). ASL regulates cellular metabolism by controlling both the levels of fumarate, a citric acid cycle intermediate, and the pool of free AMP, which affects the concentration of available ATP [48]. This is particularly important when considering the close interactions that exist between purinosomes and mitochondria. ASL is a homotetramer that contains four active sites (**Figure 8A**). Each of the four active sites are made up of residues from

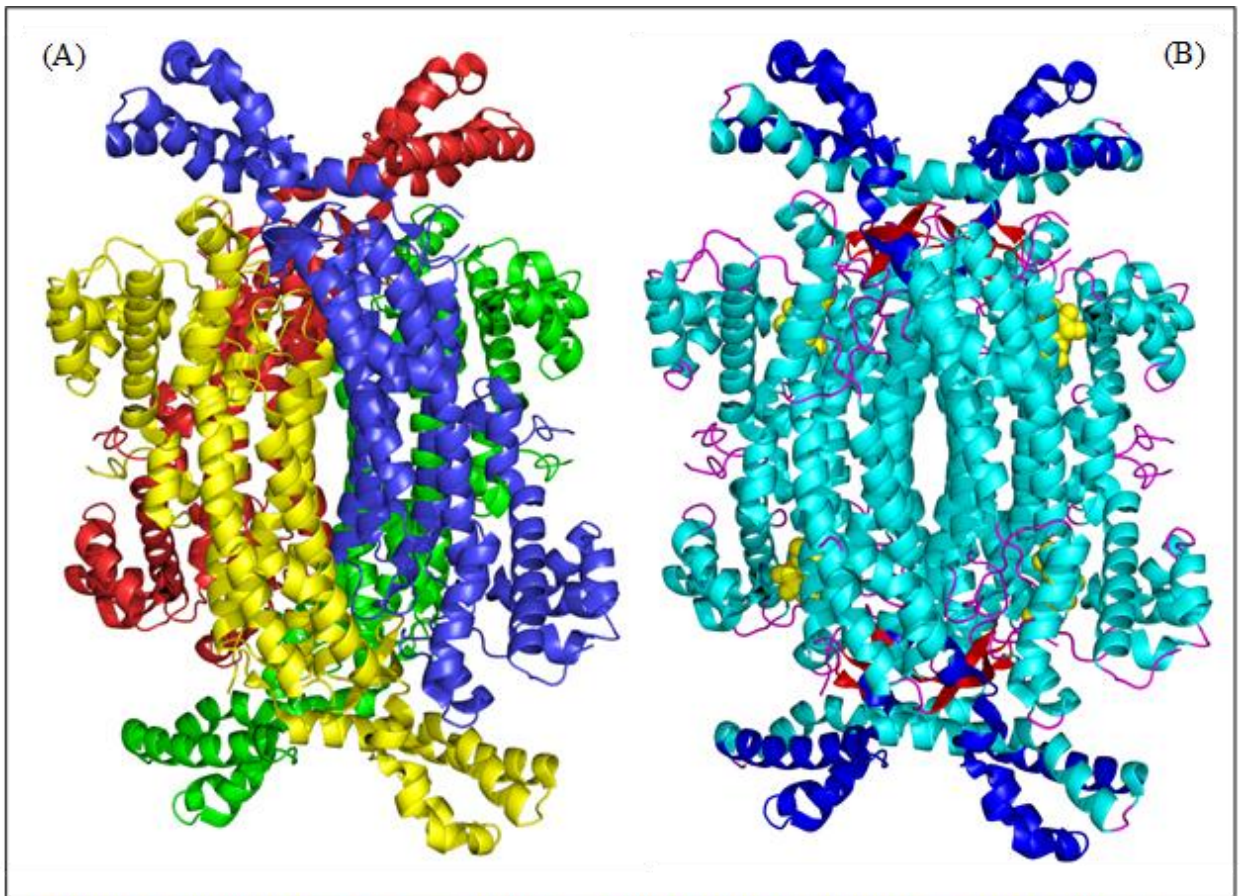

Figure 8. (A) Homotetramer of *H. sapien* ASL. Each color highlights the individual protomers of ASL. (B) AMP is bound to the enzyme in the catalytic site shown in yellow, α-helix is shown in cyan, β-sheet in red, and random coil in magenta. The deletion found in sASL is highlighted in blue. Images above created in PyMol using PDB entry 2J91.

three of the four individual protomers. It is necessary for these key residues to be positioned together for ASL to carry out catalysis [49].

ASL Mutations and Deficiencies

ASL deficiency is a result of single point mutations of the gene that often result in autistic features, mild to severe retardation, epilepsy, muscle wasting [50]. In ASL deficient patients, the substrates SAICAR and SAMP accumulate in body fluids such as cerebral spinal fluid, plasma, and urine [51]. It has been proposed that ASL deficiency is predominately correlated with structural stability and residual catalytic activity [52]. Retention of some residual ASL activity is required for the formation and stability of the purinosome for partial channeling of SAICAR through the *de novo* pathway [53, 54]. Interestingly, the majority of ASL mutations that result in loss of activity are relatively far from the active site, in the central helical region of the tetramer, which appears to be the most important for stability [55]. Many of these reported mutations result in the loss of a polar residue, suggesting that these polar regions are in part responsible for enzyme stability [55]. Mutations in this enzyme lead to neurological disorders with a varying degree of severity. Mutations affecting the structural stability of ASL affect the assembly of the purinosome *in vivo*, reduce the effectiveness of substrate channeling through the *de novo* purine biosynthetic pathway, and thus result in more severe phenotypes [52]. More than 60 cases of ASL deficiency have been reported worldwide that are a result of 45 different diseases causing mutations [45, 47]. These various mutations lead to a wide range of severity in phenotype. It has been demonstrated that *in vitro* mixing of two inactive *B. subtilis* mutant enzymes with replacements for different amino acids can lead to intersubunit complementation with a partial restoration of activity [56-58]. This intersubunit complementation and reactivation of enzyme activity was observed after mixing

and incubating E275Q with H89Q, K268Q with H89Q, and both E275Q and K268Q with H141Q [56]. *In vitro* hybridization of wild type ASL and mutant ASL has also been performed to show that wild type protomers can lead to the formation of more active and stable hybrid mixtures. These heterotetramer hybrid enzymes are advantageous to ASL deficient patients and may also be responsible for the wide range of ASL deficient phenotypes [51].

ASL Catalysis

ASL performs catalysis on SAMP and SAICAR *via* general acid-base chemistry. Kinetic studies on *B. subtilis* ASL has shown that His68 and His141 function as the general acid and base, respectively [40]. The C^{β} proton of the substrate is abstracted by the general base, yielding the carbanion intermediate [59]. In *E. coli*, the equivalent residues involved in acid-base catalysis were His91, the acid, and His171, the base, in earlier studies [60]. New insight into *E. coli* ASL enzymatic mechanism has illuminated the conserved Ser295 of the flexible loop region to act as the base (**Figure 9**) and His171 or a water molecule to likely acts as the proton donor as His91 is more than 4A away, which is too far to extract a proton from the substrate [61]. Data shows that His171 is likely the catalytic acid which coincides with the complete loss of activity during mutagenesis of this residue in *E. coli* [61]. It has been proposed that His171 functions as a catalytic

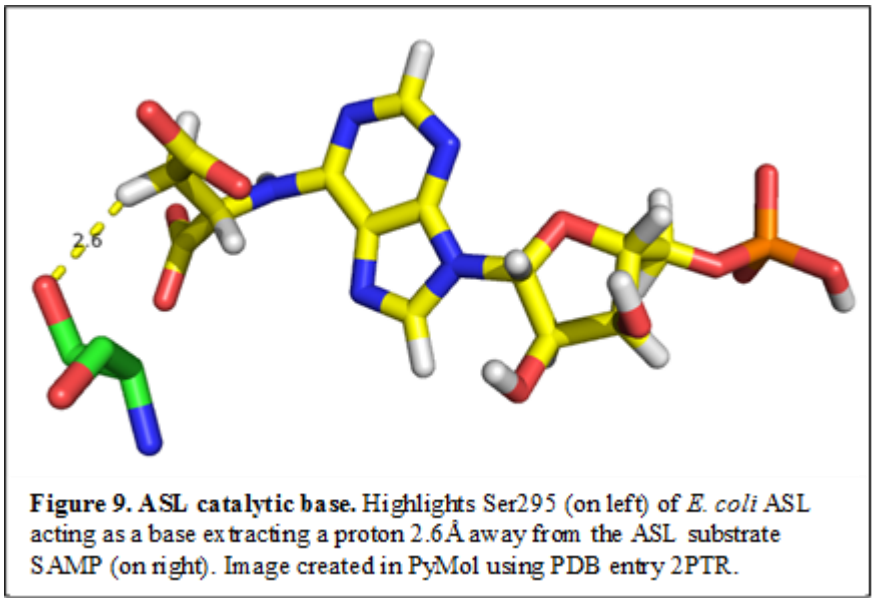

Figure 9. ASL catalytic base. Highlights Ser295 (on left) of *E. coli* ASL acting as a base extracting a proton 2.6Å away from the ASL substrate SAMP (on right). Image created in PyMol using PDB entry 2PTR.

acid *via* a charge relay interaction with Glu308, which is also conserved among the β-elimination superfamily which ASL belongs to [62]. Other members of this superfamily include aspartase [63], fumarase [64], argininosucciate lyase [65], δ -crystallin [66], and 3-carboxy-*cis*,*cis*-muconate lactonizing enzyme [67]. All of these family members are homotetramers and all have molecular weights of approximately 200 kDa [60].

Dynamic Structure of ASL

The structure of ASL appears to be dynamic, exemplified by its change in quaternary structure, when incubated at various temperatures. Analytical ultracentrifugation revealed that at 25°C, ASL exists entirely as a tetramer, whereas at 8°C and 4°C ASL dissociates into a mixture predominantly composed of monomer—dimer—trimer, with small amounts of tetramer [68]. Multimeric enzymes are typically held together by hydrophobic, electrostatic, and hydrogen bonding interactions. Hydrophobic interactions are weakened as temperature is decreased [69, 70]. ASL is no exception to this and data shows that both hydrophobic and electrostatic interactions play an essential role in ASL activity, as only the tetramer is capable of performing catalysis. There appears to be reversibility in ASL tetramer disassociation and association. The tetramer falls apart at low temperatures into a mixture of trimers, dimers, and monomer. After incubating the ASL mixture at 25°C, fully functional ASL tetramers form that regain their full activity [68]. Circular dichroism (CD) was used on the ASL low temperature mixture to assess whether ASL secondary structure changes when the tetramer disassociates. The CD spectra are nearly identical and are superimposable on the fully active tetrameric ASL at 25°C, indicating that no changes in secondary structure occurs [68]. ASL, when incubated with KBr, falls apart into a mixture of trimers, dimers, and monomers and so as a result it loses enzymatic activity, which may be attributed entirely to

the disruption of electrostatic interactions between the subunit interfaces [68]. Evidence from mutagenesis of the *B. subtilis* ASL has determined His299/Glu239 and Arg167/Asp217 appear to be the major contenders in contributing to electrostatic stability to the large surface areas of subunits A/C that contain the highest number of polar and hydrophobic residues [68]. Although the enzyme's active site is composed of residues from three different subunits [49], the tetramer must be maintained by hydrophobic and electrostatic interactions between the subunits for it to be fully active. Although these experimental temperatures are not physiologically possible, it highlights the structural changes that ASL is capable of undergoing.

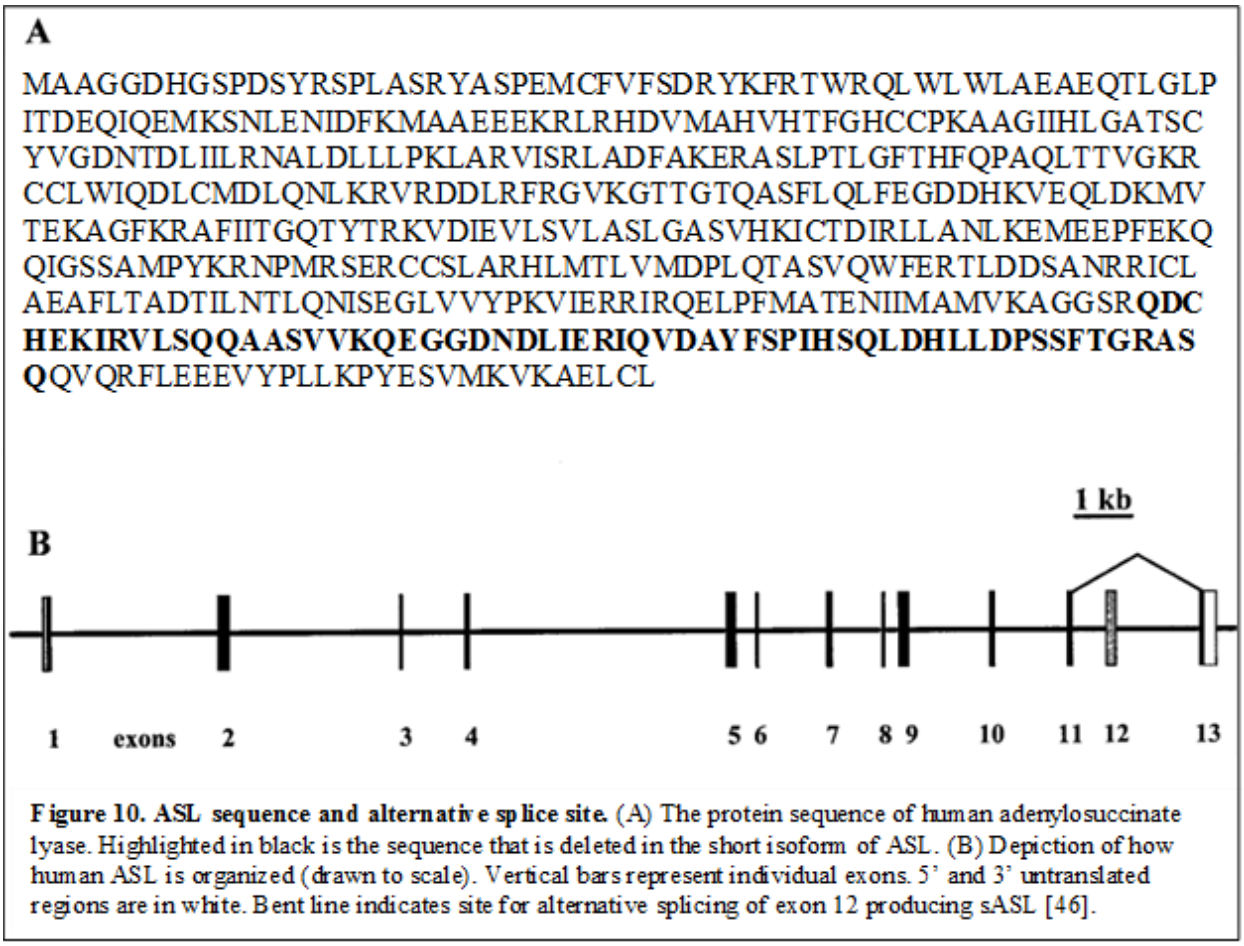

Figure 10. ASL sequence and alternative splice site. (A) The protein sequence of human adenylosuccinate lyase. Highlighted in black is the sequence that is deleted in the short isoform of ASL. (B) Depiction of how human ASL is organized (drawn to scale). Vertical bars represent individual exons. 5' and 3' untranslated regions are in white. Bent line indicates site for alternative splicing of exon 12 producing sASL [46].

Short Isoform of ASL

A short isoform of human adenylosuccinate lyase (sASL) exists that contains an internal deletion between amino acids 398 and 456 (**Figure 10A**). The short isoform, sASL, is a result of alternatively splicing around exon 12 (**Figure 10B**). This deletion in sASL is found in a non-catalytic region and does not contribute active site residues (**Figure 8B**); however, sASL does not have enzymatic function. Although present at one-tenth the levels of full-length ASL, sASL was found to be present in all tissue types tested [46]. DNA transcription and protein synthesis are energy intensive processes; therefore, it would be unlikely for the cell to produce a protein that has no function, especially in all tissues types. Human sASL is largely uncharacterized and no crystal structures of this short isoform currently exists. It has previously been stated that purinosomes are closely associated with mitochondria. During purine starvation and high purinosome formation, sASL is enriched in fractions of purified mitochondria (**Figure 11**). This observation may

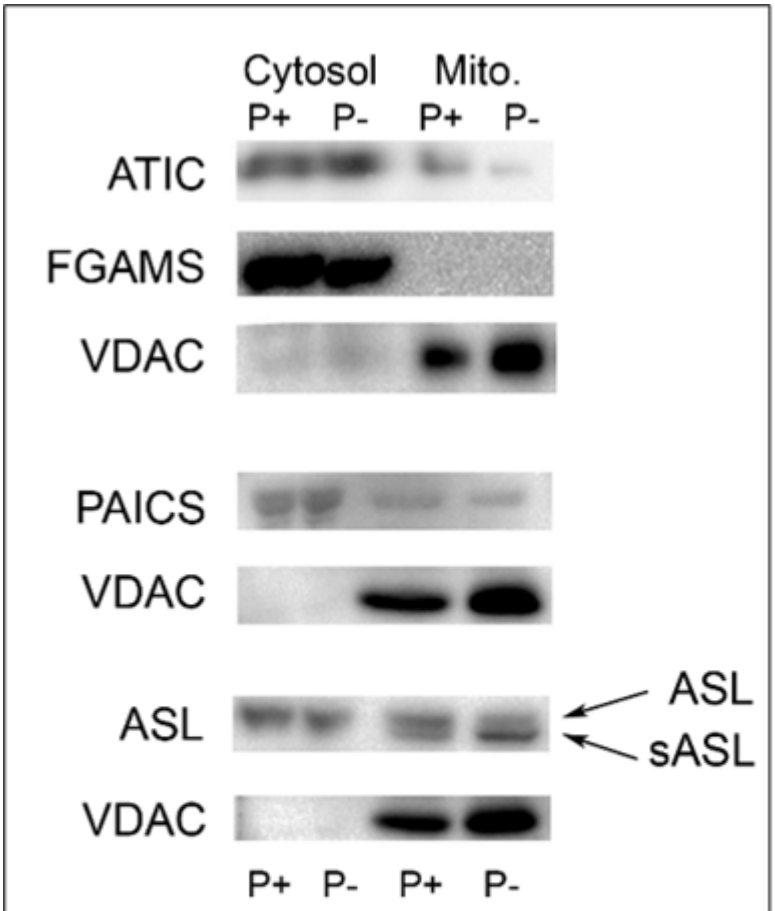

Figure 11. Western blot of purified mitochondria. Show the presence of cytoplasmic purinosome proteins including ATIC, PAICS, and ASL. VDAC is a mitochondrial protein and is only found within the organelle. FGAMS, the purinosome anchor or scaffold, is found exclusively in the cytoplasm. P+ indicates the presence of purines and low purinosome formation whereas P- represents purine starvation and high purinosome formation. The two isoforms of ASL appear with purified mitochondria. Under P- conditions, sASL is enriched in the purified mitochondrial fraction [42].

implicate a possible structural function of sASL in mediating purinosome assembly and its interactions with mitochondria.

Objectives of this Research

ASL catalyzes step 8 of the *de novo* purine biosynthetic pathway and an additional downstream reaction *en route* to the synthesis of ATP. A short isoform of this enzyme is known to be expressed in all tissues that has no enzymatic activity. Little is known about either the structure or function of this form of the protein. In order to understand the role that sASL plays in purine biosynthesis and/or the structure of the purinosome, we will investigate the structure, kinetics, and other biophysical properties of sASL. This data, and comparisons with ASL, will help to elucidate if sASL may play an important structural role in purinosome assembly and/or interaction with the mitochondria as well as modulate ASL activity.

Results and Discussion

Protein Expression and Purification

ASL and sASL were expressed under the same conditions and all proteins were purified using Ni/NTA columns and 6xHis-tags. sASL is approximately 48 kDa in size and about 50 kDa with the addition of the N-terminal 6xHis-tag. **Figure 12a** shows the expression of sASL with an appropriately sized band at 50 kDa in all cultures. A SDS-PAGE gel of sASL after purification, in **Figure 12b**, qualitatively indicates a high purity in the four most concentrated 1mL elution fractions. sASL is present in the soluble and insoluble fractions. **Figure 12c** depicts the expression of ASL with an appropriately sized band at approximately 56 kDa, which includes the N-terminal 6xHis-tag, in all of the overexpressed cultures. A SDS-PAGE gel after ASL

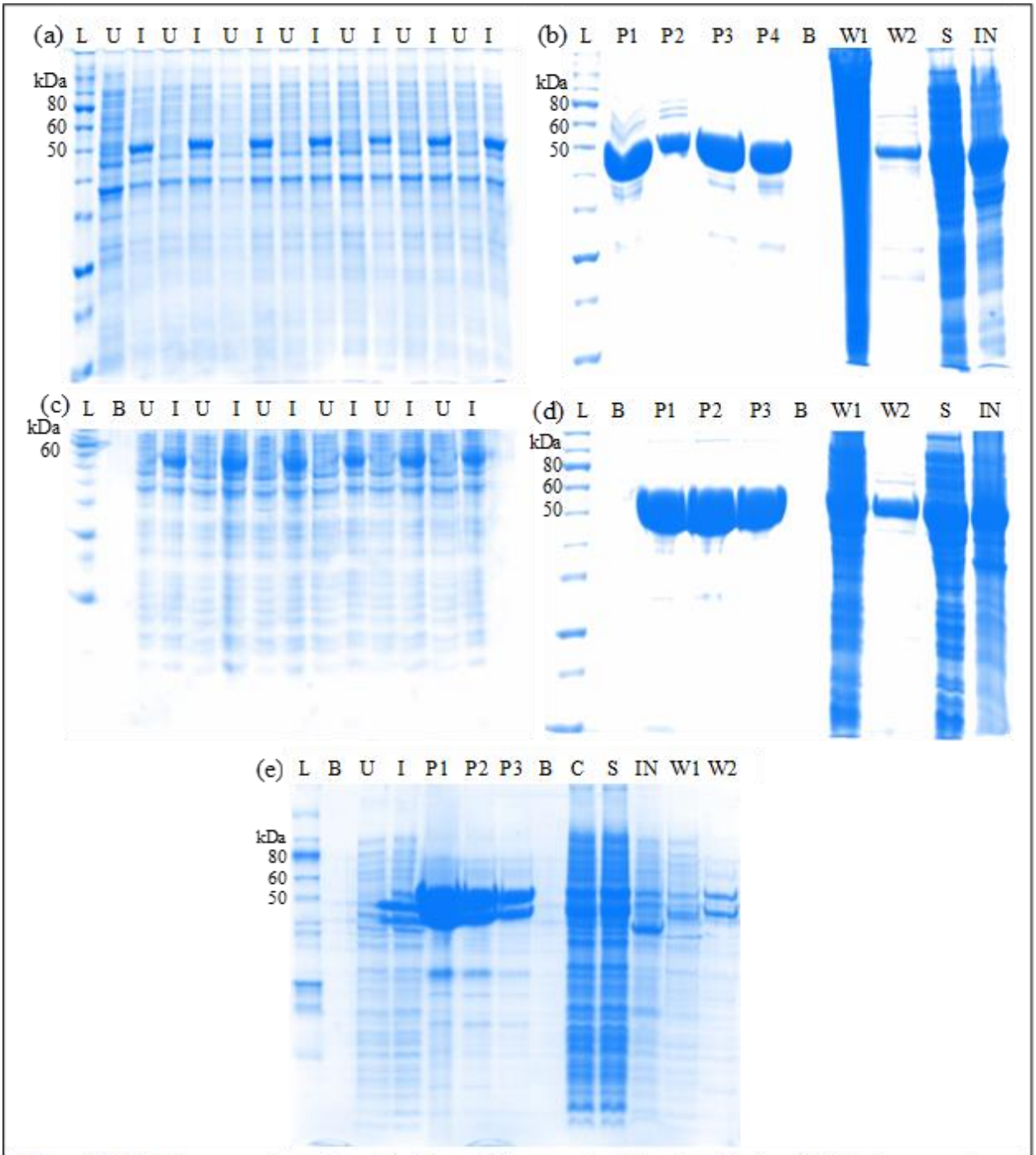

Figure 12. Protein expression and purification. sASL expression (a) and purification (b) that show correct bands at 50 kDa. ASL expression (c) and purification (d) also show correct bands at about 56 kDa. (e) ASA expression and co-purification indicate that sASL and ASL interact with each other. L is ladder, B is blank lane, U is for uninduced, I is for induced, C is for crude lysate, P is for purified fraction, W is for wash, S is for soluble fraction and IN is for insoluble fraction. All images taken on BioRad GelDoc.

purification in **Figure 12d** also qualitatively indicates the high purity of the three most

concentrated 1 mL elution fractions. As with sASL, over expressed ASL is found in both the soluble and insoluble fractions.

Active ASL exists natively as a homotetramer. As previously mentioned, mutant inactive ASL protomers can exchange with wild type protomers to produce a hybrid protein with partial restoration of activity. One putative way that sASL may function structurally is by mediating interactions between ASL and other proteins or structures such as the purinosomes. ASL and sASL may interact to form a heteromeric species that may influence ASL activity, formation of the purinosome, or interaction with mitochondria. ASL and sASL will be co-expressed to see if protomers of the two proteins form a mixed tetramer and whether this mixed protein may have physiological relevance.

ASL and sASL were successfully cloned into the pETDuet-1 vector and expressed together. ASL was bound to the N-terminal 6xHis-tag and sASL was bound to the C-terminal S-tag. **Figure 12e** shows both the expression and purification of this mixed ASLsASL protein that will be referred to as ASA. This SDS-PAGE gel indicates that both ASL and sASL are expressed together and appear at their appropriately sized bands. Purification of ASA reveals that sASL is co-purified with the 6xHis-tagged ASL. This evidence indicates that protomers of the two isoforms do indeed interact. The ratio of ASL to sASL in ASA and whether two form a tetramer or aggregate together are inconclusive; however, the data from qualitatively analyzing the SDS-PAGE gel indicates that the two may be interacting in equal amounts. The ability of protomers of ASL and sASL to interact may suggest important role in how sASL moderates ASL activity or how the purinosome complex with sASL interacts with mitochondria. As with the other two, ASA appears in both the soluble and insoluble fractions.

Size Exclusion Chromatography

As stated previously, the goals of this project are to understand if sASL plays a significant role in the regulation of ASL function, assembly of the purinosome, and/or interaction with mitochondria. Size exclusion chromatography (SEC) of the three proteins—canonical ASL,

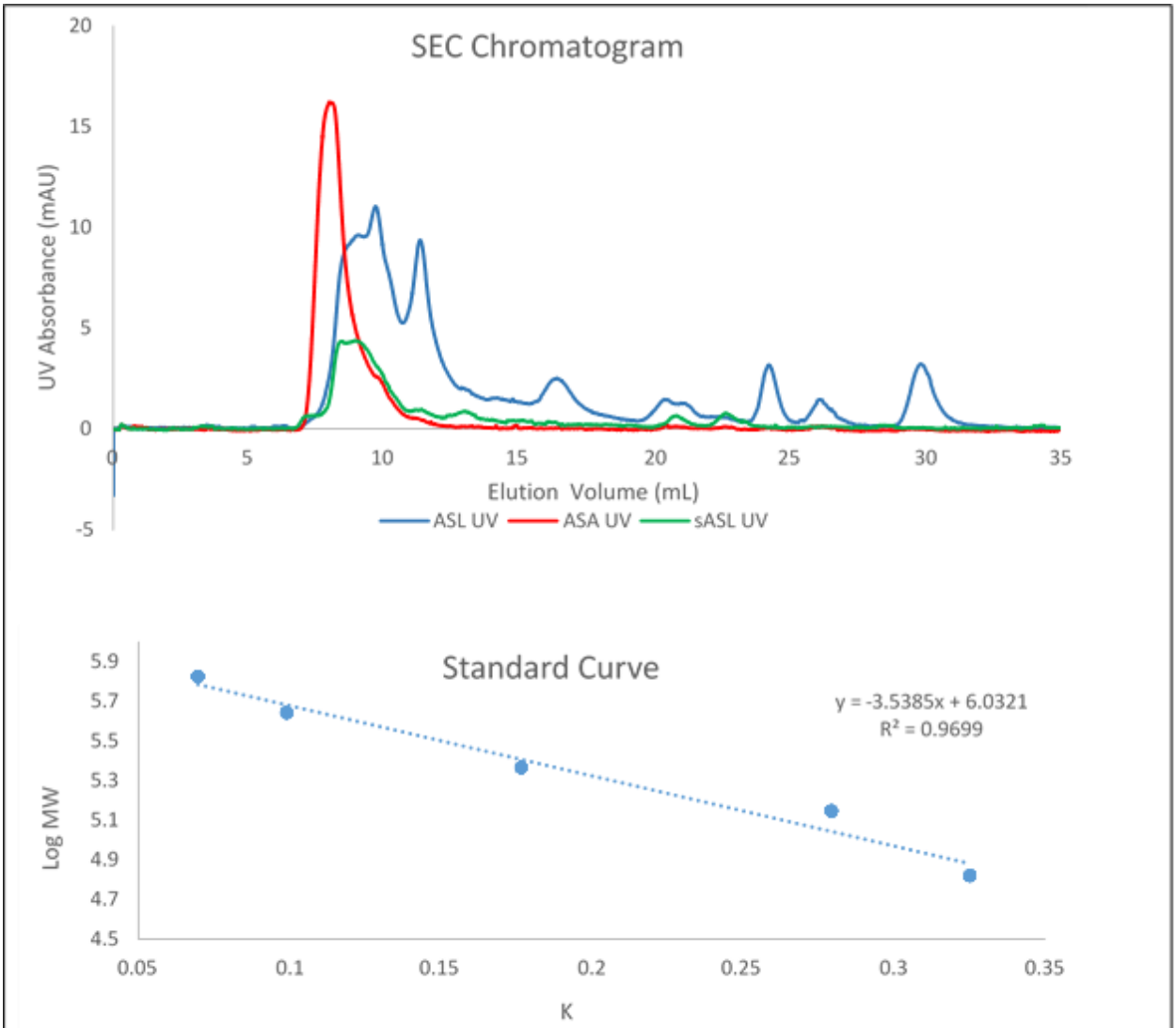

Figure 13. Size exclusion chromatography. SEC chromatogram (top) and the standard curve (bottom) determined using proteins of known size.

the short isoform sASL, and the mixed ASA—yielded inconclusive results. An expected approximate size of the ASL homotetramer is 220 kDa. As shown by the chromatogram in **Figure**

ASL		sASL		ASA	
Ve (mL)	MW (kDa)	Ve (mL)	MW (kDa)	Ve (mL)	MW (kDa)
9.06	426	8.44	580	8.0	723
9.7	310	8.99	442	9.944	275
11.36	135	11.4	133	-	-

Table 1. Molecular weights determined by SEC. Shown are the elution volumes (Ve) of each protein sample. Molecular weights (MW) of each SEC peak were determined using the linear equation given by the standard curve.

13, ASA has one large broad peak, ASL has multiple sharper peaks, and sASL has broad, less prominent peaks. **Table 1** relates the elution volume of each peak to its approximate molecular weight, none of which are around the expected size. Based off the standard curve, the molecular weights of all three of these proteins are larger than expected. ASA appears to have the largest molecular weight that appears much larger than the other two proteins alone. It may be possible that the data is simply a result of protein aggregation and precipitation; however, it may also indicate a higher order structure and oligomerization. A recent publication has suggested the ability of fibril formation as a means of regulating enzymatic function and the flux of a particular pathway [71]. CTPase synthetase (CtpS) is an example of an enzyme whose activity is regulated by the assembly of large-scale polymerized fibrils. In the case of CtpS, the accumulation of product leads to fibril formation and the inhibition of CtpS. In a similar manner, ASL may be inhibited by the short isoform *via* the formation of an oligomer, which may also mediate interaction between the purinosome and mitochondria. Further work must be conducted to determine whether the large size of the three proteins relates to their ability to form fibrils, or oligomeric structures, and whether they are physiologically relevant. It is important to note that all of the SEC runs were done at 4°C, and so it is possible that the smaller molecular weights of ASL and sASL at 135 and 133 kDa, respectively, may be a result of the dynamic structural nature of the protein to fall apart at lower temperatures into trimers, dimers, and

monomers, as previously discussed. Human ASL has previously been shown to purify as a tetramer [72], and so buffer conditions or protein precipitation may be a possible source of this inconsistency in our results.

The beta-amyloid (Aβ) peptide is an important contributor to Alzheimer's disease. Aggregation of Aβ is suspected to contribute to toxicity in neurons that leads to the trademark characteristics of the disease. A patient with Alzheimer's disease exhibits plaques in the brain with an accumulation of these Aβ fibrils. There is a direct correlation between the amount of soluble Aβ oligomers and the degree of cognitive impairment [73]. Intra and extracellular oligomers of Aβ have been found with varying molecular weights. In a study on yeast, it has been shown that the enzyme ADE12, a yeast homolog of human ASL, shows evidence of an association with Alzheimer's disease neuropathology in addition to a suggestive association with memory decline [74]. This yeast screen is inconclusive, but may suggest a link between ASL and Alzheimer's disease through fibril formation.

Stability Test and Enzyme Kinetics

ASL is very stable at room temperature in a minimal buffer unlike the short isoform which does not behave well, even at temperatures as low as 4°C. sASL is unstable and precipitates out of solution despite use of a high 400 mM NaCl buffer. In our stability test, additives were used to see what stabilized sASL and α-ketoglutarate (αKG) and fumarate proved to provide the best stabilization. 5 mM of αKG stabilized the sASL over the course of an hour at room temperature (**Figure 14**) and also stabilized the protein at 40°C over the course of 20 minutes (data not shown). However, 5 mM of αKG appears to only stabilize the protein at a concentration of 1mg/mL. A concentration higher than 1mg/mL required additional αKG to keep sASL in solution. This may

indicate that these small acids are interacting with surface residues of the protein and that a there is a ratio of molecules of acid to molecules of protein to keep it soluble. Interestingly, these two acids, αKG and fumarate, are also intermediates of the citric acid cycle that takes place in the matrix of mitochondria in eukaryotes. This, along with the enrichment of sASL in purified mitochondria (**Figure 11**), further implicates sASL as an

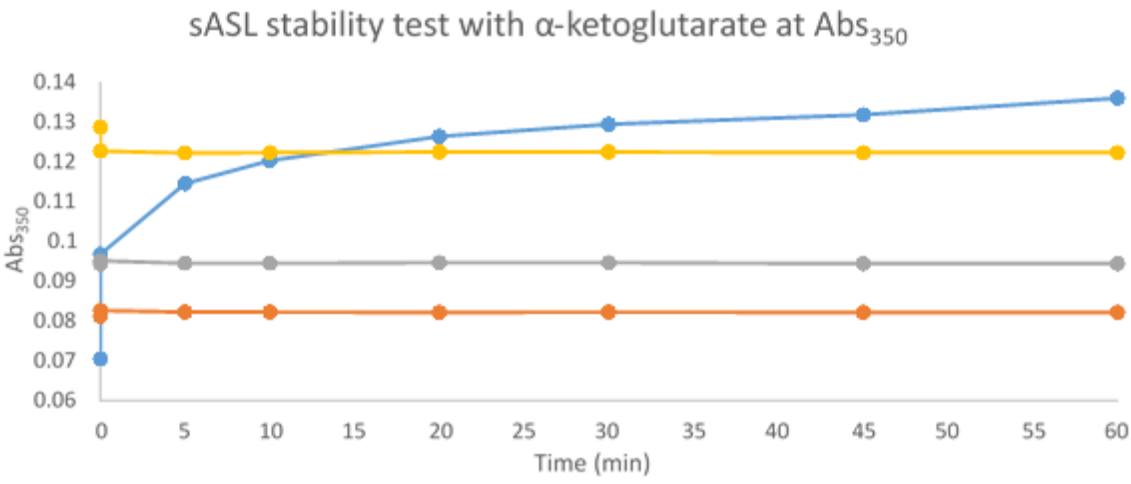

Figure 14. Stability of sASL with the addition of α-ketoglutarate.
A concentration of 5 mM αKG appears sufficient to keep sASL soluble at a concentration of 1mg/mL. Fumarate displayed similar stabilization of sASL (data not shown).

important mediator between purinosomes and mitochondria. ASA was observed to be more much stable than sASL alone. It appears that the interactions between the individual protomers of ASL and sASL provide increased structural stability, preventing the protein from precipitating quickly as with sASL. ASA behaved very well in a minimal 30 mM NaCl buffer (data not shown) at room temperature, much like canonical ASL.

ASL catalyzes step 8 of the *de novo* biosynthetic pathway, which converts SAICAR to AICAR, as well as step 2 of the purine nucleotide pathway that converts SAMP to AMP. SAMP has a strong absorbance at 282 nm whereas AMP absorbs very little at this wavelength (**Figure 15**). Fumarate did not absorb at 282 nm. This provided an effective means of monitoring the

conversion of SAMP to AMP and fumarate. 100 µM of SAMP and 10 mg of enzyme were used in each run. sASL has been confirmed to have no enzymatic activity with the substrate SAMP.

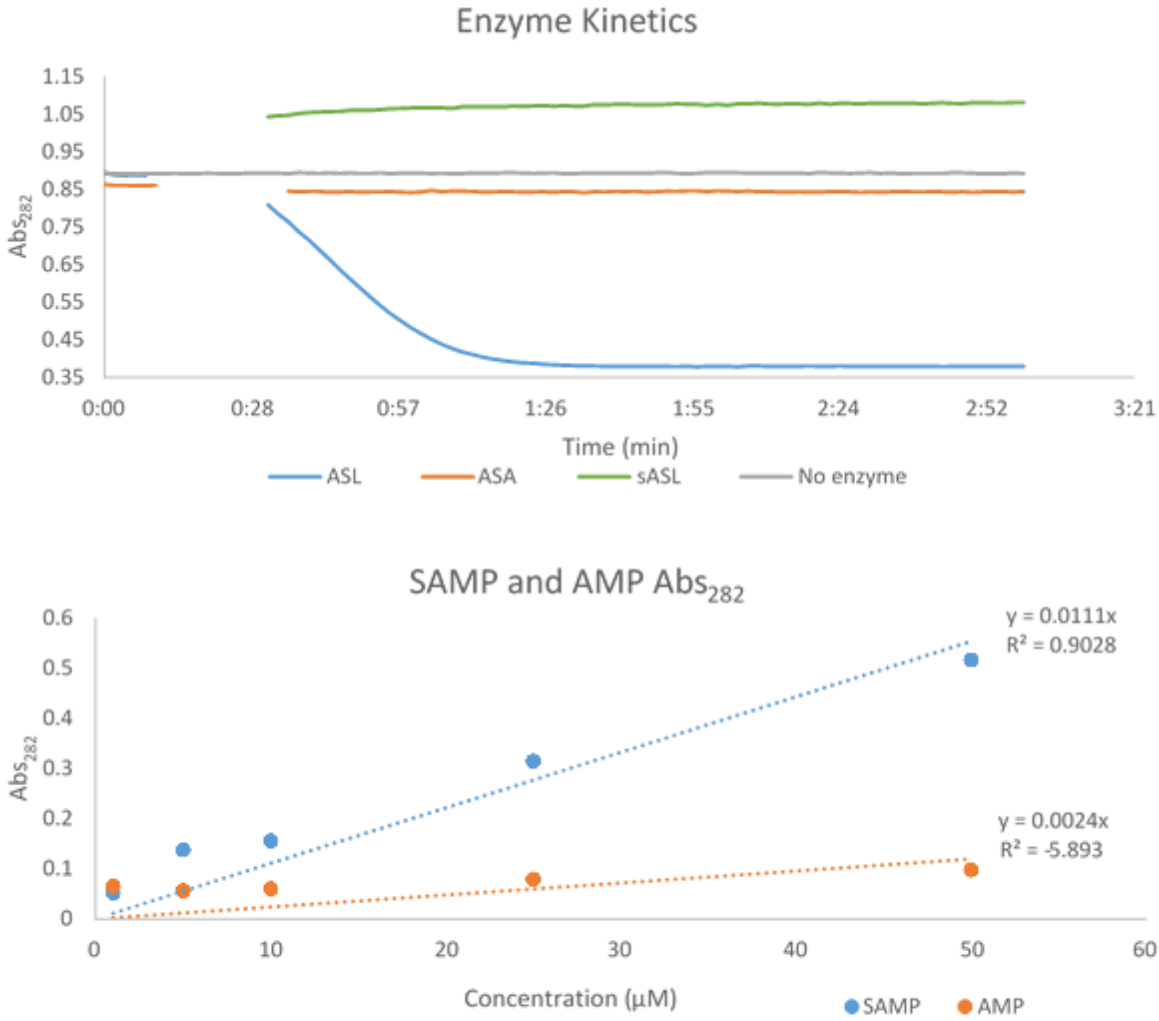

Figure 15. Enzyme kinetics. Assessed by measuring at Abs_{282} (top). Among the three proteins, only ASL shows enzymatic activity. ASA does not show partial recovery in activity, but does remain stable. sASL absorbance increases upon addition of enzyme indicating that the protein still experiences stability issues, but does level off shortly after. The gap in each line is a result of stopping the reading to add 10 mg of enzyme. SAMP and AMP absorbance at 282 nm (bottom) was measured with various concentrations and plotted to obtain the molar absorbtivity (ε) of SAMP.

Addition of sASL yielded an increase in absorbance indicating that the protein still experiences instability and likely requires additional αKG in future tests of its kinetics. ASA also does not convert SAMP to AMP, but does remain in solution and stable over the course of the kinetic assay. It appears that ASL protomers do not give the heteromeric protein a partial restoration of activity.

The absorbance spectrum (**Figure 15**) was used to acquire the molar absorbtivity (ε) of SAMP which was calculated to be 0.0111 $L\ mol^{-1}\ cm^{-1}$. The Beer-Lambert law was used to determine the concentration of SAMP at a given absorbance during the kinetic test of ASL. The rate of reaction in conversion of SAMP to AMP was determined to be 1.075676 M/s at room temperature.

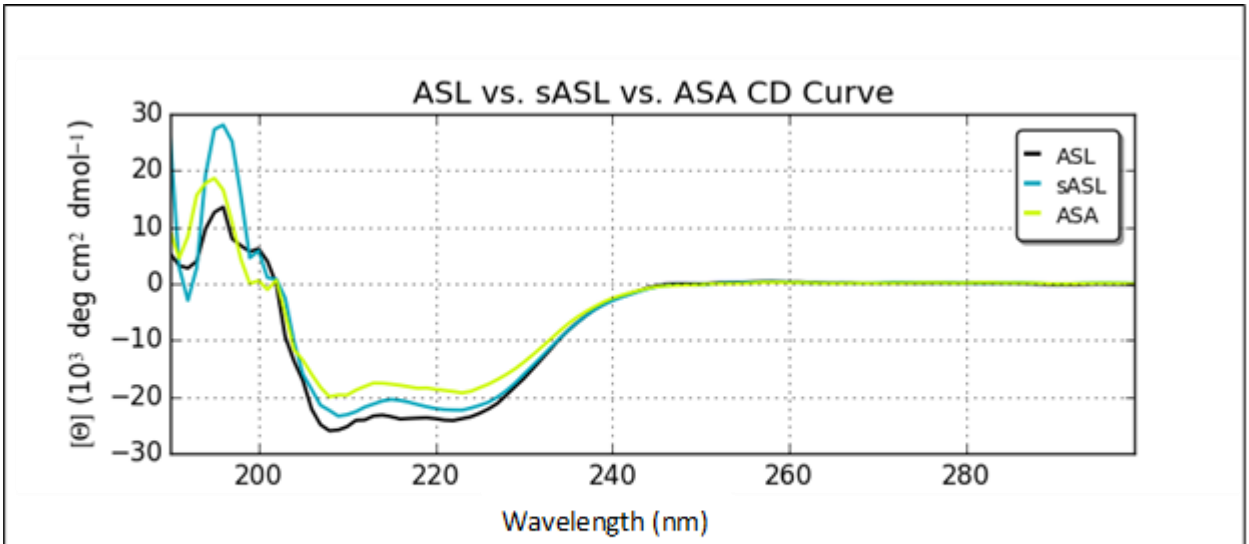

Figure 16. Circular dichroism spectra. There appears to be a shift in the spectrum of sASL in comparison to the other two proteins that may indicate a change in the secondary structure as a result of the internal deletion.

Circular Dichroism

Circular Dichroism (CD) was used to determine if the deletion in sASL changes the secondary structure of the protein. It has yet to be determined what kind of structural change occurs as a result of the internal deletion in sASL as there is no known crystal structure of the protein. The CD spectra comparison of ASL, sASL, and ASA (**Figure 16**) show that there is a shift in the spectrum of sASL which indicates a change in its secondary structure. According to the CAPITO CD analyzing tool [75], there are slight differences in the secondary structures of ASL and sASL with the major difference being the increase in random coil. This may be an indication as to why sASL is less stable than full length ASL in a minimal salt solution. Based off of the ASA spectrum, the CAPITO tool indicated that the α-helical, β-sheet, and random coil values landed between ASL

and sASL. This suggests that protomers of the two proteins simply mix and do not affect each other's secondary structure by interacting.

Crystallization

One of the primary goals of this project is to find conditions that produce crystals of sASL that would be used to solve the structure using X-ray crystallography. Doing so would help elucidate what role sASL may have and what morphological changes occur as a result of the internal deletion previously mentioned. It was not until the addition of αKG to the buffer that drops with sASL yielded anything except precipitated protein and salt crystals. Two conditions in the JCSG Core II screen, 16 and 20, generated drops with clear spots surrounded by some precipitated protein. The conditions used were 0.2M $MgCl_2$, 0.1M imidazole pH 8, and either 35% or 40% v/v MPD. These two conditions were further optimized by changing the amount of MPD and pH of the solution. The optimization was done using in a 24-well plate and, with larger 2.5µL drops, revealed that there were clear objects with sharp edges at the center of each spot. The clear objects appeared to be plates with varying degrees of depth. Each object was immediately surrounded by a sphere of clear solution, much like an oil droplet, in the midst of protein precipitate. It was determined qualitatively that the condition 0.2M $MgCl_2$, 0.1M imidazole pH 8, and 45% v/v MPD produced the largest objects. Further data must be collected to determine if the objects are indeed protein crystals or salt crystals. JB Screen Classic 1, 3, 6, and 7, QIAGEN Classic Suite 1-4, Hampton Crystal Screen 1-2, and Hampton PEG/Ion Screen 1-2 were all tested prior to the addition of αKG to stabilize sASL in solution. It would be beneficial to repeat the above mentioned screens with sASL stabilized by αKG to determine if there are other potential crystal producing conditions. The Hampton SaltRx 1-2 and JCSG Core I screens produced no favorable conditions despite the

use of αKG stabilized sASL. In addition, the heteromeric ASA has become an interesting target for crystallization. A crystal structure of ASA would elucidate the interactions that occur between ASL and sASL subunits. Two conditions from the JCSG Core II screen show interesting results, but requires further optimization.

Conclusion

Purines are necessary components of all life and are used in DNA replication, RNA synthesis, in high energy molecules, as signaling molecules, and as cofactors. Purines are created by the *de novo* biosynthetic pathway and recycled by the salvage pathway. Both pathways are active at the same time; however, the *de novo* pathway is upregulated when the cell demands a higher level of purines. In humans, the 10 steps of the biosynthetic pathway are carried out by six multifunctional enzymes. The purinosome is an agglomerate of these enzymes that forms during an increased demand for purines that has also been shown to interact with mitochondria. Clustering of these enzymes increases flux by a phenomena known as proximity channeling. ASL is a member of the biosynthetic pathway with a short isoform that has no enzymatic function. sASL is expressed in all tissue types and is thought to play a structural role in purinosome assembly and/or mediator with mitochondria.

sASL has been co-purified with mitochondria suggesting that it may play an important role between the purinosome and mitochondria. sASL has also been co-purified with the canonical ASL showing that the two do indeed interact, which may have physiological relevance. sASL is unstable in solution, but becomes stable with the addition of small acids that are found as intermediates in the citric acid cycle that occurs in the matrix of mitochondria. When sASL is expressed with ASL, the resulting mixed ASA is very stable. Both sASL and ASA do not have

enzymatic activity. SEC shows that sASL and ASA run large in comparison to canonical ASL. It is possible that interaction of sASL with ASL produces a stable, soluble, functional aggregate or fibril. CD data reveals that there are slight structural differences between ASL and sASL, including an increase in random coil. CD shows that expressing the two proteins together does not make a structural change in one or the other.

sASL may drive ASL to oligomerize with itself and perhaps interact with other cellular components such as mitochondria. sASL seems to play a structural role in its ability to drive higher order structure with full length ASL and may modulate activity by doing so. This oligomerization may be relevant for purinosome assembly and disassembly, purinosome related diseases, and/or interaction with mitochondria. sASL may dictate the equilibrium of active ASL and also between tetramer and fibril. Further tests must be conducted to verify whether the heteromeric ASA is indicative of a higher order structure such as a fibril or polymer driven by sASL. Dynamic light scattering or SEC coupled to multiangle light scattering would be potential tools for additional investigation.

Methods and Materials

Cloning ASL, sASL and mixed ASLsASL

IDT primers were used to amply the sASL gene. Restriction enzymes BamHI-HF and Xho I were used to digest sASL and vector. ASL was received from the laboratory of Stephen J. Benkovic. ASL was amplified using a separate set of IDT primers and the gene and vector were digested with restrictions enzymes EcoR I and Xho I. Ligations were carried out overnight at 4°C. DH5α cells were transformed using the above ligated constructs and a standard transformation protocol. Both constructs were sequenced using T7 promotor and T7 terminator to ensure they

were in frame with the 6xHis-tag. In order to express ASL and sASL together, the pETDuet-1 vector was acquired, which has two multiple cloning sites. Initially, sASL was digested and inserted into the second MCS using restriction enzymes EcoR V and Xho I. ASL was subsequently digested and inserted into the first MCS of the sASL-pETDuet-1 vector using EcoR I and Sal I. Ligations were carried out at 4°C overnight and DH5α cells were used for transformation. Sequencing data confirmed that ASL was in frame with the N-terminal 6xHis-tag and that sASL was in frame with the C-terminal S-tag.

Expression of ASL-pTHT, sASL-pTHT and ASLsASL-pETDuet-1

All three constructs, ASL-pTHT, sASL-pTHT, and ASLsASL-pETDuet-1 were transformed into BL21 (DE3) cells and expressed in 1 liter of Luria broth (LB). Each liter of LB was inoculated with 10 mL of overnight culture grown at 37°C in LB with antibiotic—kanamycin for ASL-pTHT and sASL-pTHT and ampicillin for ASLsASL-pETDuet-1. All of the large scale cultures were grown at 37°C and induced at 18°C with IPTG with an OD of approximately 0.6. No antibiotics were used for large scale growth. ASL-pTHT and sASL-pTHT were induced with 0.5mM IPTG whereas ASLsASL-pETDuet-1 was induced with 0.1mM IPTG. All protein expression and folding was allowed to carry on at 18°C for five hours before spinning down at 5180g and 4°C to form cell pellets that were then frozen at -80°C.

Purification of ASL, sASL, and mixed ASLsASL (ASA)

Lysis buffer, composed of 50mM sodium phosphate pH 7.6, 300mM NaCl, and 10mM imidazole, was used to re-suspend pellets, which were then lysed by five, one minute rounds of sonication with a power output of 7 and a duty cycle of 50%. Cell lysates were then spun down at 30,996g and 4°C and the resulting soluble fraction was collected. IMAC was used to purify ASL, sASL, and ASA on a 1 mL Ni/NTA His-trap FF column using the AKTA FPLC system. A flow

rate of 1mL/min was used throughout the purification process. After the column was loaded with sample, a first wash using lysis buffer was performed followed by a second wash with 25mM imidazole. 250mM imidazole was then used for the elution of each protein. Purity was assessed qualitatively by SDS-PAGE. Econo-Pac 10DG desalting gravity columns were used to buffer exchange each of the proteins into a suitable buffer. ASL was buffer exchanged into a storage buffer of 10mM Hepes pH 7, 50mM NaCl, 2mM DTT, and 10% glycerol. sASL was buffer exchanged into 10mM Tris pH 7.6, 30mM NaCl, and 50mM alpha–ketoglutarate. ASA was buffer exchanged into 10mM Tris pH 7.5 and 30mM NaCl. None of the 6xHis-tags were cleaved off to perform the experiments mentioned. ASL, sASL, and ASA were concentrated in 10k Macrosep Advance Centrifugal Devices by Pall at 3234g and 4°C to concentrations of 5.6mg/mL, 10mg/mL, and 9.5mg/mL, respectively. Aliquots of each protein were flash frozen with liquid nitrogen and stored at -80°C. All gel images taken by BioRad GelDoc.

Size Exclusion Chromatography

A Superdex 200 increase 10/200 GL column was used to perform size exclusion chromatography on ASA, ASL, and sASL all in a 10 mM Tris pH 7, 400 mM NaCl buffer. Each protein sample was diluted in 100 μL of the buffer and injected at a concentration of approximately 2-3 mg/mL. The column was used on the AKTA FPLC system at a constant flow rate of 0.5 mL/min. Thyroglobulin (669 kDa), ferritin (440 kDa), catalase (232 kDa), lactate dehydrogenase (140 kDa), and albumin (66 kDa) are proteins of known size that were ran on the column to establish a standard curve that was used to estimate the molecular weights of ASA, ASL, and sASL. UNICORN control software was used to identify the elution volumes of the standard proteins as well as the unknown protein samples. K was determined by the equation $K =$

$(Ve - Vo)/(Vt - Vo)$ where Ve is the elution volume, Vt is the total column volume, and Vo is the void volume.

Kinetics and Stability

A SpectraMAX Plus UV and fluorescent plate reader was used to measure the stability of sASL and ASA and to test the kinetics of each protein in the presence of the substrate SAMP. Absorbance was measured at 282 nm to observe the conversion of SAMP to AMP. A 10 mM Hepes pH7, 400 mM NaCl buffer was used in all runs testing enzyme kinetics with a total volume of 400 µL in a quartz cuvette. 100 µM SAMP and 10 mg of enzyme were used in each run. Each test was run three times in succession and an average was taken. The rate was calculated by measuring the change in SAMP concentration over time with the calculated ε of 0.0111 $L\ mol^{-1}\ cm^{-1}$.

A 96-well plate was used to measure absorbance at 350 nm to observe protein precipitation in two different concentrated salt buffers that would indicate its stability. Sodium fumarate and α-ketoglutarate were used as additives to stabilize sASL at room temperature over the course of an hour and at 40°C over the course of 20 minutes. Both additives were tested at concentrations of 1, 5, 10, 25, and 50 mM in 30 mM and 200 mM NaCl buffers at a total volume of 100 µL and with sASL at a concentration of approximately 1 mg/mL for each run. Both stability data and kinetic data were plotted in Excel to generate curves.

Circular Dichroism

The OLIS RSM 1000 was used to analyze the secondary structure of ASL, sASL, and ASA. All samples were buffer exchanged into 10 mM sodium acetate pH 7 and 400 mM NaCl and concentrated to 0.5 mg/mL. A cuvette with a path length of 1 mm and 250 µL of sample at a concentration of 0.5mg/mL was used for each run. 10 runs were done in succession and the data

points were averaged. Each run was done between 190—310 nm with 240 data points. CAPITO CD analyzing and plotting tool was used to generate CD curves and to determine a percentage of alpha helical, beta sheet, and random coil content in each of the three proteins.

Crystallography

JB Screen Classic 1, 3, 6, and 7, QIAGEN Classic Suite 1-4, Hampton Crystal Screen 1-2, and Hampton PEG/Ion Screen 1-2 were all done by hand in 24 well plates using the hanging drop method. Each drop consisted of 1.25 µL protein and 1.25 µL of well solution with a total well volume of 350 µL. The Hampton SaltRx 1-2 and JCSG Core I and II screens were done on an Art Robbins Instruments Phoenix robot using the sitting drop method in 96-well ARI intelli-plates with 0.3 µL of protein and 0.3 µL of well solution. All trays were incubated at 18°C.

References

1. Rosemeyer, H., *The chemodiversity of purine as a constituent of natural products.* Chem Biodivers, 2004. **1**(3): p. 361-401.
2. Halpern, B.P., *What's in a name? Are MSG and umami the same?* Chem Senses, 2002. **27**(9): p. 845-6.
3. Drury, A.N. and A. Szent-Gyorgyi, *The physiological activity of adenine compounds with especial reference to their action upon the mammalian heart.* J Physiol, 1929. **68**(3): p. 213-37.
4. Hasko, G., et al., *Adenosine receptors: therapeutic aspects for inflammatory and immune diseases.* Nat Rev Drug Discov, 2008. **7**(9): p. 759-70.
5. Travain, M.I. and J.P. Wexler, *Pharmacological stress testing.* Semin Nucl Med, 1999. **29**(4): p. 298-318.
6. Guimaraes, P.M. and J. Londesborough, *The adenylate energy charge and specific fermentation rate of brewer's yeasts fermenting high- and very high-gravity worts.* Yeast, 2008. **25**(1): p. 47-58.
7. Gourine, A.V., et al., *ATP is a mediator of chemosensory transduction in the central nervous system.* Nature, 2005. **436**(7047): p. 108-11.
8. Molz, S., et al., *GMP prevents excitotoxicity mediated by NMDA receptor activation but not by reversal activity of glutamate transporters in rat hippocampal slices.* Brain Res, 2008. **1231**: p. 113-20.
9. Fredholm, B.B., *Adenosine, an endogenous distress signal, modulates tissue damage and repair.* Cell Death Differ, 2007. **14**(7): p. 1315-23.
10. Junger, W.G., *Immune cell regulation by autocrine purinergic signalling.* Nat Rev Immunol, 2011. **11**(3): p. 201-12.
11. Di Virgilio, F., *Purines, purinergic receptors, and cancer.* Cancer Res, 2012. **72**(21): p. 5441-7.
12. von Kugelgen, I. and T.K. Harden, *Molecular pharmacology, physiology, and structure of the P2Y receptors.* Adv Pharmacol, 2011. **61**: p. 373-415.
13. Ferrari, D., et al., *The P2X7 receptor: a key player in IL-1 processing and release.* J Immunol, 2006. **176**(7): p. 3877-83.
14. Schenk, U., et al., *ATP inhibits the generation and function of regulatory T cells through the activation of purinergic P2X receptors.* Sci Signal, 2011. **4**(162): p. ra12.
15. Chen, C.C., et al., *A P2X purinoceptor expressed by a subset of sensory neurons.* Nature, 1995. **377**(6548): p. 428-31.
16. Cook, S.P. and E.W. McCleskey, *Cell damage excites nociceptors through release of cytosolic ATP.* Pain, 2002. **95**(1-2): p. 41-7.
17. Vlaskovska, M., et al., *P2X3 knock-out mice reveal a major sensory role for urothelially released ATP.* J Neurosci, 2001. **21**(15): p. 5670-7.
18. Rong, W., et al., *Pivotal role of nucleotide P2X2 receptor subunit of the ATP-gated ion channel mediating ventilatory responses to hypoxia.* J Neurosci, 2003. **23**(36): p. 11315-21.
19. Costa, F. and I. Biaggioni, *Role of nitric oxide in adenosine-induced vasodilation in humans.* Hypertension, 1998. **31**(5): p. 1061-4.
20. Murad, F., *Shattuck Lecture. Nitric oxide and cyclic GMP in cell signaling and drug development.* N Engl J Med, 2006. **355**(19): p. 2003-11.

21. Delghandi, M.P., M. Johannessen, and U. Moens, *The cAMP signalling pathway activates CREB through PKA, p38 and MSK1 in NIH 3T3 cells.* Cell Signal, 2005. **17**(11): p. 1343-51.
22. Conti, M., D. Mika, and W. Richter, *Cyclic AMP compartments and signaling specificity: role of cyclic nucleotide phosphodiesterases.* J Gen Physiol, 2014. **143**(1): p. 29-38.
23. Insel, P.A., et al., *Cyclic AMP is both a pro-apoptotic and anti-apoptotic second messenger.* Acta Physiol (Oxf), 2012. **204**(2): p. 277-87.
24. Mayevsky, A. and E. Barbiro-Michaely, *Use of NADH fluorescence to determine mitochondrial function in vivo.* Int J Biochem Cell Biol, 2009. **41**(10): p. 1977-88.
25. Lee, J., et al., *Regulator of fatty acid metabolism, acetyl coenzyme a carboxylase 1, controls T cell immunity.* J Immunol, 2014. **192**(7): p. 3190-9.
26. Castellana, M., et al., *Enzyme clustering accelerates processing of intermediates through metabolic channeling.* Nat Biotechnol, 2014. **32**(10): p. 1011-8.
27. Huang, X., H.M. Holden, and F.M. Raushel, *Channeling of substrates and intermediates in enzyme-catalyzed reactions.* Annu Rev Biochem, 2001. **70**: p. 149-80.
28. Dueber, J.E., et al., *Synthetic protein scaffolds provide modular control over metabolic flux.* Nat Biotechnol, 2009. **27**(8): p. 753-9.
29. Deng, Y., et al., *Mapping protein-protein proximity in the purinosome.* J Biol Chem, 2012. **287**(43): p. 36201-7.
30. Ginsburg, A. and E.R. Stadtman, *Multienzyme systems.* Annu Rev Biochem, 1970. **39**: p. 429-72.
31. Hrazdina, G. and R.A. Jensen, *Spatial organization of enzymes in plant metabolic pathways.* Annual Review of Plant Biology, 1992. **43**(1): p. 241-267.
32. Narayanaswamy, R., et al., *Widespread reorganization of metabolic enzymes into reversible assemblies upon nutrient starvation.* Proc Natl Acad Sci U S A, 2009. **106**(25): p. 10147-52.
33. Smith, G.K., et al., *Characterization of the enzyme complex involving the folate-requiring enzymes of de novo purine biosynthesis.* Biochemistry, 1980. **19**(18): p. 4313-21.
34. An, S., et al., *Reversible compartmentalization of de novo purine biosynthetic complexes in living cells.* Science, 2008. **320**(5872): p. 103-6.
35. Liechti, G. and J.B. Goldberg, *Helicobacter pylori relies primarily on the purine salvage pathway for purine nucleotide biosynthesis.* J Bacteriol, 2012. **194**(4): p. 839-54.
36. French, J.B., et al., *Hsp70/Hsp90 chaperone machinery is involved in the assembly of the purinosome.* Proc Natl Acad Sci U S A, 2013. **110**(7): p. 2528-33.
37. Becker, M.A. and M. Kim, *Regulation of purine synthesis de novo in human fibroblasts by purine nucleotides and phosphoribosylpyrophosphate.* J Biol Chem, 1987. **262**(30): p. 14531-7.
38. Matsui, H., et al., *gsk disruption leads to guanosine accumulation in Escherichia coli.* Biosci Biotechnol Biochem, 2001. **65**(5): p. 1230-5.
39. Shimaoka, M., et al., *Effects of edd and pgi disruptions on inosine accumulation in Escherichia coli.* Biosci Biotechnol Biochem, 2005. **69**(7): p. 1248-55.
40. Zhang, Y., M. Morar, and S.E. Ealick, *Structural biology of the purine biosynthetic pathway.* Cell Mol Life Sci, 2008. **65**(23): p. 3699-724.
41. An, S., et al., *Microtubule-assisted mechanism for functional metabolic macromolecular complex formation.* Proc Natl Acad Sci U S A, 2010. **107**(29): p. 12872-6.

42. French, J.B., et al., *Purinosomes Exhibit mTOR-mediated Functional Association with Mitochondria.* Submitted, 2014.
43. Fon, E.A., et al., *Mapping of the human adenylosuccinate lyase (ADSL) gene to chromosome 22q13.1-->q13.2.* Cytogenet Cell Genet, 1993. **64**(3-4): p. 201-3.
44. Stone, R.L., et al., *A mutation in adenylosuccinate lyase associated with mental retardation and autistic features.* Nat Genet, 1992. **1**(1): p. 59-63.
45. Lee, P. and R.F. Colman, *Expression, purification, and characterization of stable, recombinant human adenylosuccinate lyase.* Protein Expr Purif, 2007. **51**(2): p. 227-34.
46. Kmoch, S., et al., *Human adenylosuccinate lyase (ADSL), cloning and characterization of full-length cDNA and its isoform, gene structure and molecular basis for ADSL deficiency in six patients.* Hum Mol Genet, 2000. **9**(10): p. 1501-13.
47. Ray, S.P., et al., *Structural and biochemical characterization of human adenylosuccinate lyase (ADSL) and the R303C ADSL deficiency-associated mutation.* Biochemistry, 2012. **51**(33): p. 6701-13.
48. Van den Berghe, G., et al., *The purine nucleotide cycle and its molecular defects.* Prog Neurobiol, 1992. **39**(5): p. 547-61.
49. Brosius, J.L. and R.F. Colman, *Three subunits contribute amino acids to the active site of tetrameric adenylosuccinate lyase: Lys268 and Glu275 are required.* Biochemistry, 2002. **41**(7): p. 2217-26.
50. Ciardo, F., C. Salerno, and P. Curatolo, *Neurologic aspects of adenylosuccinate lyase deficiency.* J Child Neurol, 2001. **16**(5): p. 301-8.
51. De Zoysa Ariyananda, L., et al., *In vitro hybridization and separation of hybrids of human adenylosuccinate lyase from wild-type and disease-associated mutant enzymes.* Biochemistry, 2011. **50**(8): p. 1336-46.
52. Baresova, V., et al., *Mutations of ATIC and ADSL affect purinosome assembly in cultured skin fibroblasts from patients with AICA-ribosiduria and ADSL deficiency.* Hum Mol Genet, 2012. **21**(7): p. 1534-43.
53. Vliet, L.K., et al., *Molecular characterization of the AdeI mutant of Chinese hamster ovary cells: a cellular model of adenylosuccinate lyase deficiency.* Mol Genet Metab, 2011. **102**(1): p. 61-8.
54. Zikanova, M., et al., *Biochemical and structural analysis of 14 mutant adsl enzyme complexes and correlation to phenotypic heterogeneity of adenylosuccinate lyase deficiency.* Hum Mutat, 2010. **31**(4): p. 445-55.
55. Spiegel, E.K., R.F. Colman, and D. Patterson, *Adenylosuccinate lyase deficiency.* Mol Genet Metab, 2006. **89**(1-2): p. 19-31.
56. Lee, T.T., et al., *His68 and His141 are critical contributors to the intersubunit catalytic site of adenylosuccinate lyase of Bacillus subtilis.* Biochemistry, 1999. **38**(1): p. 22-32.
57. Segall, M.L., M.A. Cashman, and R.F. Colman, *Important roles of hydroxylic amino acid residues in the function of Bacillus subtilis adenylosuccinate lyase.* Protein Sci, 2007. **16**(3): p. 441-8.
58. Segall, M.L. and R.F. Colman, *Gln212, Asn270, and Arg301 are critical for catalysis by adenylosuccinate lyase from Bacillus subtilis.* Biochemistry, 2004. **43**(23): p. 7391-402.
59. Bulusu, V., et al., *Elucidation of the substrate specificity, kinetic and catalytic mechanism of adenylosuccinate lyase from Plasmodium falciparum.* Biochim Biophys Acta, 2009. **1794**(4): p. 642-54.

60. Toth, E.A. and T.O. Yeates, *The structure of adenylosuccinate lyase, an enzyme with dual activity in the de novo purine biosynthetic pathway.* Structure, 2000. **8**(2): p. 163-74.
61. Tsai, M., et al., *Substrate and product complexes of Escherichia coli adenylosuccinate lyase provide new insights into the enzymatic mechanism.* J Mol Biol, 2007. **370**(3): p. 541-54.
62. Kozlov, G., et al., *The structure of phosphate-bound Escherichia coli adenylosuccinate lyase identifies His171 as a catalytic acid.* Acta Crystallogr Sect F Struct Biol Cryst Commun, 2009. **65**(Pt 9): p. 857-61.
63. Shi, W., et al., *The structure of L-aspartate ammonia-lyase from Escherichia coli.* Biochemistry, 1997. **36**(30): p. 9136-44.
64. Weaver, T.M., et al., *The multisubunit active site of fumarase C from Escherichia coli.* Nat Struct Biol, 1995. **2**(8): p. 654-62.
65. Turner, M.A., et al., *Human argininosuccinate lyase: a structural basis for intragenic complementation.* Proc Natl Acad Sci U S A, 1997. **94**(17): p. 9063-8.
66. Simpson, A., et al., *The structure of avian eye lens delta-crystallin reveals a new fold for a superfamily of oligomeric enzymes.* Nat Struct Biol, 1994. **1**(10): p. 724-34.
67. Williams, S.E., et al., *3-Carboxy-cis,cis-muconate lactonizing enzyme from Pseudomonas putida is homologous to the class II fumarase family: a new reaction in the evolution of a mechanistic motif.* Biochemistry, 1992. **31**(40): p. 9768-76.
68. De Zoysa Ariyananda, L. and R.F. Colman, *Evaluation of types of interactions in subunit association in Bacillus subtilis adenylosuccinate lyase.* Biochemistry, 2008. **47**(9): p. 2923-34.
69. Oakenfull, D. and D. Fenwick, *Thermodynamics and mechanism of hydrophobic interaction.* Australian Journal of Chemistry, 1977. **30**(4): p. 741-752.
70. Southall, N.T., K.A. Dill, and A. Haymet, *A view of the hydrophobic effect.* The Journal of Physical Chemistry B, 2002. **106**(3): p. 521-533.
71. Barry, R.M., et al., *Large-scale filament formation inhibits the activity of CTP synthetase.* Elife, 2014. **3**: p. e03638.
72. Stone, R.L., H. Zalkin, and J.E. Dixon, *Expression, purification, and kinetic characterization of recombinant human adenylosuccinate lyase.* J Biol Chem, 1993. **268**(26): p. 19710-6.
73. Lue, L.F., et al., *Soluble amyloid beta peptide concentration as a predictor of synaptic change in Alzheimer's disease.* Am J Pathol, 1999. **155**(3): p. 853-62.
74. Treusch, S., et al., *Functional links between Abeta toxicity, endocytic trafficking, and Alzheimer's disease risk factors in yeast.* Science, 2011. **334**(6060): p. 1241-5.
75. Wiedemann, C., P. Bellstedt, and M. Gorlach, *CAPITO--a web server-based analysis and plotting tool for circular dichroism data.* Bioinformatics, 2013. **29**(14): p. 1750-7.